PD IEC/TR 62048:2014

BSI Standards Publication

Optical fibres — Reliability — Power law theory

...making excellence a habit.™

National foreword

This Published Document is the UK implementation of IEC/TR 62048:2014. It supersedes PD IEC/TR 62048:2011 which is withdrawn.

The UK participation in its preparation was entrusted by Technical Committee GEL/86, Fibre optics, to Subcommittee GEL/86/1, Optical fibres and cables.

A list of organizations represented on this committee can be obtained on request to its secretary.

This publication does not purport to include all the necessary provisions of a contract. Users are responsible for its correct application.

Published by BSI Standards Limited 2014

ISBN 978 0 580 82512 5
ICS 33.180.10

Compliance with a British Standard cannot confer immunity from legal obligations.

This Published Document was published under the authority of the Standards Policy and Strategy Committee on 28 February 2014.

Amendments/corrigenda issued since publication

Date	Text affected

PD IEC/TR 62048:2014

IEC TR 62048

Edition 3.0 2014-01

TECHNICAL REPORT

colour inside

Optical fibres –
Reliability – Power law theory

INTERNATIONAL
ELECTROTECHNICAL
COMMISSION

PRICE CODE XB

ICS 33.180.10

ISBN 978-2-8322-1369-8

Warning! Make sure that you obtained this publication from an authorized distributor.

CONTENTS

INTERNATIONAL ELECTROTECHNICAL COMMISSION

OPTICAL FIBRES –

Reliability – Power law theory

FOREWORD

1) The International Electrotechnical Commission (IEC) is a worldwide organization for standardization comprising all national electrotechnical committees (IEC National Committees). The object of IEC is to promote international co-operation on all questions concerning standardization in the electrical and electronic fields. To this end and in addition to other activities, IEC publishes International Standards, Technical Specifications, Technical Reports, Publicly Available Specifications (PAS) and Guides (hereafter referred to as "IEC Publication(s)"). Their preparation is entrusted to technical committees; any IEC National Committee interested in the subject dealt with may participate in this preparatory work. International, governmental and non-governmental organizations liaising with the IEC also participate in this preparation. IEC collaborates closely with the International Organization for Standardization (ISO) in accordance with conditions determined by agreement between the two organizations.
2) The formal decisions or agreements of IEC on technical matters express, as nearly as possible, an international consensus of opinion on the relevant subjects since each technical committee has representation from all interested IEC National Committees.
3) IEC Publications have the form of recommendations for international use and are accepted by IEC National Committees in that sense. While all reasonable efforts are made to ensure that the technical content of IEC Publications is accurate, IEC cannot be held responsible for the way in which they are used or for any misinterpretation by any end user.
4) In order to promote international uniformity, IEC National Committees undertake to apply IEC Publications transparently to the maximum extent possible in their national and regional publications. Any divergence between any IEC Publication and the corresponding national or regional publication shall be clearly indicated in the latter.
5) IEC itself does not provide any attestation of conformity. Independent certification bodies provide conformity assessment services and, in some areas, access to IEC marks of conformity. IEC is not responsible for any services carried out by independent certification bodies.
6) All users should ensure that they have the latest edition of this publication.
7) No liability shall attach to IEC or its directors, employees, servants or agents including individual experts and members of its technical committees and IEC National Committees for any personal injury, property damage or other damage of any nature whatsoever, whether direct or indirect, or for costs (including legal fees) and expenses arising out of the publication, use of, or reliance upon, this IEC Publication or any other IEC Publications.
8) Attention is drawn to the Normative references cited in this publication. Use of the referenced publications is indispensable for the correct application of this publication.
9) Attention is drawn to the possibility that some of the elements of this IEC Publication may be the subject of patent rights. IEC shall not be held responsible for identifying any or all such patent rights.

The main task of IEC technical committees is to prepare International Standards. However, a technical committee may propose the publication of a technical report when it has collected data of a different kind from that which is normally published as an International Standard, for example "state of the art".

IEC/TR 62048, which is a technical report, has been prepared by subcommittee 86A: Fibres and cables, of IEC technical committee 86: Fibre optics.

This third edition cancels and replaces the second edition published in 2011, and constitutes a technical revision.

The main changes with respect to the previous edition are listed below:

– correction to the unit of failure rates in Table 1;

– correction to the FIT equation for instantaneous failure rate [19][1] in addition to all call-outs and derivations;
– insertion of a new note about fibre length dependency of failure rates;
– addition of informative Annex A and relevant reference;
– editorial corrections of inconsistencies.

The text of this technical report is based on the following documents:

Enquiry draft	Report on voting
86A/1537/DTR	86A/1554/RVC

Full information on the voting for the approval of this technical report can be found in the report on voting indicated in the above table.

This publication has been drafted in accordance with the ISO/IEC Directives, Part 2.

The committee has decided that the contents of this publication will remain unchanged until the stability date indicated on the IEC web site under "http://webstore.iec.ch" in the data related to the specific publication. At this date, the publication will be

- reconfirmed,
- withdrawn,
- replaced by a revised edition, or
- amended.

A bilingual version of this publication may be issued at a later date.

IMPORTANT – The 'colour inside' logo on the cover page of this publication indicates that it contains colours which are considered to be useful for the correct understanding of its contents. Users should therefore print this document using a colour printer.

1 Numbers in square brackets refer to the Bibliography.

INTRODUCTION

Reliability is expressed as an expected lifetime or as an expected failure rate. The results cannot be used for specifications or for the comparison of the quality of different fibres. This technical report develops the theory behind the experimental principles used in measuring the fibre parameters needed in the reliability formulae. Much of the theory is taken from the referenced literature and is presented here in a unified manner. The primary results are formulae for lifetime or for failure rate, given in terms of the measurable parameters. Conversely, an allowed maximum service stress or extreme value of another parameter may be calculated for an acceptable lifetime or failure rate.

For readers interested only in the final results of this technical report – a summary of the formulae used and numerical examples in the calculation of fibre reliability – Clauses 6 and 7 – are sufficient and self-contained. Readers wanting a detailed background with algebraic derivations will find this in Clauses 8 to 12. An attempt is made to unify the approach and the notation to make it easier for the reader to follow the theory. Also, it should ensure that the notation is consistent in all test procedures. The Bibliography has a limited set of mostly theoretical references, but it is not necessary to read them to follow the analytical development in this technical report. Annex A introduces a statistical strength degradation (SSD) map which gives intuitive understanding of the physical meaning of the formulae appearing in Clauses 10 and 11.

NOTE Clauses 8 to 12 reference the B-value, and this is done for theoretical completeness only. There are as yet no agreed methods for measuring B, so the Bibliography gives only a brief analytical outline of some proposed methods and furthermore develops theoretical results for the special case in which B can be neglected.

OPTICAL FIBRES –

Reliability – Power law theory

1 Scope

This technical report is a guideline that gives formulae to estimate the reliability of fibre under a constant service stress based on a power law for crack growth.

NOTE Power law is derived empirically, but there are other laws which have a more physical basis (for example, the exponential law). All these laws generally fit short-term experimental data well but lead to different long-term predictions. The power law has been selected as a most reasonable representation of fatigue behaviour by the experts of several standard-formulating bodies.

2 Normative references

The following documents, in whole or in part, are normatively referenced in this document and are indispensable for its application. For dated references, only the edition cited applies. For undated references, the latest edition of the referenced document (including any amendments) applies.

IEC 60793-1-30, *Optical fibres – Part 1-30: Measurement methods and test procedures – Fibre proof test*

IEC 60793-1-31, *Optical fibres – Part 1-31: Measurement methods and test procedures – Tensile strength*

3 Symbols

Table 1 provides a list of symbols found in this report. Each symbol appears in the subclause(s) indicated in the final column of the table.

Table 1 – Symbols

Symbol	Unit	Name	Subclause
a	µm	Flaw depth	8.1
a_f	µm	Radius of glass fibre	11.3
B	GPa^2×s	Crack strength preservation parameter or B-value	8.1
B_0	GPa^2×s	Transitional B-value at the slow-unloading/fast-unloading boundary	10.4
c	Dimensionless	Non-linearity term for stress versus strain	8.4
C	Dimensionless	Additive dimensionless proof test term or C-value	11.6
C_0	Dimensionless	Transitional value of C at the slow-unloading/fast-unloading boundary	11.6
D	Mm	Fibre-axes separation in two-point bending	11.3.3
E_0	Gpa	Zero-strain Young's modulus	8.4
F	Dimensionless	Fibre failure probability	12.1
$K_I(t)$	GPa×µ$m^{1/2}$	Stress intensity factor	8.1
K_{Ic}	GPa×µ$m^{1/2}$	Critical stress intensity factor	8.1

Symbol	Unit	Name	Subclause
L	km	Fibre effective length under uniform stress, or equivalent tensile length	11.2.1
L_b	km	Fibre length in uniform bend	11.3.2
L_p	km	Mean survival length, or survival length, during proof-testing	11.6
L_0	km	Gauge length, reference length	11.2.1
m	Dimensionless	"Inert" Weibull parameter or m-value	11.2.1
m_d	Dimensionless	m-value under dynamic fatigue	11.5
m_s	Dimensionless	m-value under static fatigue	11.4
n	Dimensionless	Stress corrosion susceptibility parameter or n-value	6.3, 8.1
N_p	km^{-1}	Mean break rate per unit length during proof-testing	11.6
$N(S)$	km^{-1}	Flaws per unit length not exceeding inert strength S	11.2.1
P	Dimensionless	Fibre survival probability	11.2.1
P_p	Dimensionless	Fibre survival probability after proof-testing	11.6
R	M	Fibre bend radius	11.3.2
$S(t)$	GPa	"Inert" strength of a crack	8.1
S_p	GPa	Strength after proof-testing	10.3
S_{pmin}	GPa	Minimum strength after proof-testing	10.4
S_0	GPa	Weibull gauge strength	11.2.1
t	s	Variable of time	8.1
t_d	s	Time to failure under dynamic fatigue	8.3.2
		Dwell time of proof test	6.3.2, 6.4.2, 10.2, 10.3
t_f	s	Lifetime (time to failure) under constant stress or static fatigue testing	8.2, 9.2
t_{fp}	s	Lifetime after proof-testing	11.8
t_{fpmin}	s	Minimum lifetime for certain survival after proof-testing	11.8
$t_f(1)$	Dimensionless	Intercept on a static fatigue plot	9.2
t_l	ms	Loading time of proof test	10.2
t_p	ms	Effective proof test time	10.3
t_u	ms	Unloading time of proof test	10.2
t_0	Dimensionless	Static Weibull time-scaling parameter	11.4
V	µm/s	Crack growth velocity	8.1
V_C	µm/s	Critical crack growth velocity	8.1
x	Dimensionless	Factor relating bend length to equivalent tensile length	11.3.2
Y	Dimensionless	Crack geometry shape parameter	8.1
α	Dimensionless	Ratio of unloading parameters of proof test to crack parameters	10.4
β	$GPa^n \times s \times km^{(n-2)/m}$	Weibull β-value	11.4, 11.5
ε	Dimensionless	Strain corresponding to a particular stress	8.4
λ_i	s^{-1}	Instantaneous failure rate	12.1
λ_a	s^{-1}	Averaged failure rate	12.2
$\sigma(t)$	GPa	Stress applied to a crack	8.1
σ_a	GPa	Applied stress under static fatigue testing and service time	9.2, 12.2
$\dot{\sigma}_a$	GPa/s	Applied stress rate under dynamic fatigue testing	8.3.2

Symbol	Unit	Name	Subclause
σ_f	GPa	Failure stress under dynamic fatigue testing, without proof-testing	8.3.2
σ_{fp}	GPa	Failure stress after proof-testing	11.8
σ_{fpmin}	GPa	Minimum failure stress after proof-testing	11.8
$\sigma_f(1)$	Dimensionless	Intercept on a dynamic fatigue plot	8.3.2
σ_p	GPa	Proof test stress	10.2
σ_0	GPa	Dynamic Weibull stress-scaling parameter	11.5

4 General approach

First, the equivalence of the growth of an individual crack and its associated weakening is shown. This is related to applied stress or strain as an arbitrary function of time. Applied stress can be taken to fracture, from which the lifetime of the crack is calculated. Next, the destructive tests of static and dynamic fatigue are reviewed, along with their relationship to each other. These tests measure parameters useful in the theory. This also shows the difference between "inert" strength and "dynamic" strength.

The above single-crack theory is then extended to a statistical distribution of many cracks. This is done in terms of a survival (or failure) Weibull probability distribution in strength. It can allow for several deployment geometries in testing and service. The inert distribution and the distributions obtained by static or dynamic fatigue testing are derived for before and after proof-testing. The latter is sometimes done with approximations that may not require knowing the B-value explicitly. Finally, the various parameters measured by the above testing are related to formulae for fibre reliability, that is, lifetime and failure rate.

Some of the main assumptions in the development are as indicated below.

– The relationship between the stress intensity factor, applied stress, and flaw size is given by Equation (29); while at fracture, the relationship between the critical stress intensity factor, strength, and flaw depth is given by Equation (30).

– The crack growth velocity is related to the stress intensity factor by Equation (32).

– The Weibull distribution of stress (before any proof-testing) is unimodal according to Equations (85) and (86), or bimodal according to Equation (91). The (m, S_0) pair appropriate to the desired survival probability level and length shall be used. Deployment lengths will differ upon the application such as fibre on reels, in cable, splice trays, or within a connector or other component. Because of the low failure probabilities desired, however, the low-strength extrinsic mode must usually be used.

– The values of the fatigue parameters, both static and dynamic, depend upon the fibre environment, fibre ageing and fibre preconditioning prior to testing. In theory, they are taken to be independent of time, so that some engineering judgement is needed to decide the practical values to be used in the calculations. This also implies that the corresponding static and dynamic fatigue parameters equal each other (for the same environment and time duration).

– Zero-stress ageing is not accounted for. Since the above parameters are independent of time, the strength decreases due only to stress fatigue following the power law according to 8.1.

5 Formula types

The formulae utilize parameters obtained from fatigue testing-to-failure, and from proof-testing with potential random failures. In the service condition of interest, a fibre of effective length L (dependent upon deployment geometry) is subjected to a constant applied service stress that does not change with time. (This stress is tensile, including bending stress. Torsional or compressive stresses are not covered.) The lifetime as a function of failure probability or failure rate as a function of time are given.

The formulae assume a Weibull distribution with parameters that vary among fibre types and perhaps among fibres of the same type. Moreover, they change with environment and applied stress levels. The Weibull distribution may have several nominally linear terms depending upon several levels of flaw strength. It is important that the Weibull parameters for the term of interest be used in the formulae. These are obtained from fatigue measurements. Generally, the low-strength region near the proof test stress and below is of interest, and measurements shall be on long fibre gauge lengths and with many samples, so that the total fibre length tested is large. Parameters measured for a small number of short samples, characterizing the high-strength region, will differ from the preceding ones. They shall not be used in the formulae to extrapolate to lower-strength lower-probability regions.

Within the above power law assumptions, the equations in Clauses 8 to 12 are algebraically "exact". However, in some applications, certain terms may be negligible, and more approximate and simpler algebraic equations are given in Clause 13. This has the advantage in that the B-value, for which there is yet no standard test method and which has been reported to span several orders of magnitude, is not required.

Even with these formulae, there is no assured way of accurately predicting fibre reliability. Some fibres may break before the most conservative of predictions, while others may last longer than the most pessimistic of predictions. After fibre manufacture, fatigue or damage may occur due to cabling, installation, or operation; this usually cannot be accounted for in the theory. A start on estimating these effects could be made by measuring the parameters of fibres after each of these stages, but this is not commonly done.

For convenience in assisting the reader to find the derivations of equations, if desired, the formulae summarized in Clauses 6 and 7 include the indication in brackets of the equations listed in Clauses 8 to 13. However, it is not necessary to refer to the derivations to be able to follow Clauses 6 and 7.

6 Measuring parameters for fibre reliability

6.1 Overview

This clause outlines how the parameters in the reliability (lifetime and failure rate) equations are obtained in the approximation of the small B-value. Proof test parameters are obtained from testing the full length of fibre to be deployed. By contrast, both static and dynamic fatigue procedures use many short-length test samples. These are used to obtain "linear" Weibull plots of the cumulative failure probability F scaled as $\ln\text{-}\ln\frac{1}{P}$ (where $P = 1 - F$ is the survival probability) versus the ln of a suitable variable (failure time or failure stress). For situations in which the plot may be fitted to two or more straight line parts, that part closest to the anticipated service stress should be used in obtaining the needed parameters.

6.2 Length and equivalent length

The testing and service geometries may differ from each other. The symbol L_0 is the gauge length in static or dynamic fatigue testing, whereas L is the in-service length subjected to constant applied service stress. The gauge length equals the actual length only for the case of longitudinal tension. Other geometries require equivalent lengths.

For uniform bending (for example, mandrel wrap), the in-service bend length L_b is replaced by an approximate equivalent in-service tensile length L given by Equation (97).

$$L \approx 0{,}4 \frac{L_b}{\sqrt{x}} \tag{1}$$

The same relationship holds between the gauge bend length L_{b0} and the equivalent gauge length L_0. In this equation there is the factor of Equation (98), i.e.

$$x = \frac{mn}{n-2} = m_s n = \frac{m_d n}{n+1} \tag{2}$$

using inert, static fatigue, and dynamic fatigue parameters, respectively, as obtained below.

For two-point bending, the equivalent length depends upon the applied stress in a complex way. Computation of the equivalent in-service length for an arbitrary applied service stress is difficult. The equivalent gauge length is approximately 10 μm to 30 μm, depending upon the failure stress.

6.3 Reliability parameters

6.3.1 Overview

This subclause outlines methods that are commonly used to derive reliability parameters.

6.3.2 Proof-testing

– Obtain the composite proof test parameter $\sigma_p^n t_p$, where σ_p is the actual proof test stress during dwell, and n is the stress-corrosion susceptibility parameter (or n-value). The effective proof test time is given by Equation (64), i.e.

$$t_p = t_d + \frac{t_l + t_u}{n+1} \tag{3}$$

obtained from the loading time t_l, the dwell time t_d, and the unloading time t_u.

– (Optional) If from proof-testing the mean number of breaks N_p per length or the mean survival length L_p during proof-testing is known, calculate Equations (172) and (173), i.e.

$$\beta = \frac{\sigma_p^n t_p}{N_p^{\frac{n-2}{m}}} = \sigma_p^n t_p L_p^{\frac{n-2}{m}} \tag{4}$$

$$\text{where } \frac{m}{n-2} = m_s = \frac{m_d}{n+1} \tag{5}$$

If this is not possible, obtain β as a fitting parameter in 6.3.3, 6.3.4, or 6.4.

6.3.3 Static fatigue

– Obtain the static Weibull plot of scaled probability versus the natural logarithm of failure times t_f for any particular constant applied stress σ_a [Equation (174)]

$$\ln \frac{1}{P_p(t_f)} = \left[\left(t_f \sigma_a^n + t_p \sigma_p^n \right)^{m_s} - \left(t_p \sigma_p^n \right)^{m_s} \right] \frac{L}{\beta^{m_s}} \tag{6}$$

– Determine parameters ms and β from the characteristics of the plot.

– Obtain the best-fit straight line to the logarithm of failure times versus the logarithm of applied stresses (see Equation (48))

$$\lg t_f(\sigma_a) \approx \lg t_f(1) - n \lg \sigma_a \tag{7}$$

Measure the static stress-corrosion susceptibility parameter as the negative slope $-n$ of this line. The term $t_f(1)$ is the "intercept" of this line on the ordinate axis, that is, the value of failure time where the applied stress is unity. (This value will depend on the units used, and may require a straight-line extrapolation beyond the data points. It does not have the dimension of time.)

6.3.4 Dynamic fatigue

IEC 60793-1-31 describes how to measure both short-length and long-length strength distributions of optical fibres.

– Obtain the dynamic Weibull plot of scaled probability versus the natural logarithm of failure stresses σ_f for any particular constant applied stress rate $\dot{\sigma}_a$ (see Equation (175))

$$\ln \frac{1}{P_p(\sigma_f)} = \left\{ \left[\frac{\sigma_f^{n+1}}{(n+1)\dot{\sigma}_a} + \sigma_p^n \, t_p \right]^{\frac{m_d}{n+1}} - \left(\sigma_p^n \, t_p \right)^{\frac{m_d}{n+1}} \right\} \frac{L}{\beta^{\frac{m_d}{n+1}}} \tag{8}$$

Determine parameters m_d and β from the characteristics of the plot.

– Obtain the best-fit straight line to the logarithm of failure stresses versus the logarithm of applied stress rates, as given in Equation (53):

$$\lg \sigma_f(\dot{\sigma}_a) \approx \lg \sigma_f(1) + \frac{\lg \dot{\sigma}_a}{n+1} \tag{9}$$

Measure the dynamic stress-corrosion susceptibility parameter from the slope $\frac{1}{n+1}$ of this line.

The term $\sigma_f(1)$ is the "intercept" of this line on the ordinate axis, that is, the value of failure stress where the applied stress rate is unity. (This value will depend on the units used, and may require a straight-line extrapolation beyond the data points. It does not have the dimension of stress.)

6.4 Parameters for the low-strength region

6.4.1 Overview

This subclause describes the way to measure the strength distribution at sufficiently low probability to represent the distribution of failure strengths near the proof test stress level for the second mode of the Weibull distribution (shown as the extrinsic region in Figure 14). Normally, the fibre population has been proof-tested once according to Clause 10.

NOTE These implementations are used only for characterization and not for specification.

6.4.2 Variable proof test stress

This method (briefly mentioned in 10.5) subjects a full length of fibre to a certain proof test stress, another length to a higher proof test stress, and so on for several increasing levels of proof test stress. The mean survival length L_p (or number of breaks N_p per unit length) is counted for each length and stress level. This resembles a static fatigue test in which the failure stress (the proof test stress σ_p) varies. However, the failure time does not exceed the fixed proof test time t_p. The n-values are obtained by the fatigue measurements of 6.3.

First, consider the case in which there is no initial proof test at manufacture. From Equations (171) and (173) one has

$$\ln L_p + m_s(n \ln \sigma_p + \ln t_p - \ln \beta) = 0 \tag{10}$$

so a logarithmic plot of mean survival length versus proof test stress should be close to a straight line. The slope is $-nm_s$, while the stress and length "intercepts" are $\frac{1}{n}(\ln \beta - \ln t_p)$ and $m_s(\ln t_p - \ln \beta)$, respectively.

In Reference [11], fibres with a 400 µm jacket and initial lengths of 10 km to 15 km were used, with five proof test strains of 0,8 % to 3,5 %. There was no other initial proof test. Equation (10) is equivalent to Equations (18) to (20) of Reference [11] with $C = \beta^{-m_s}$. With a dwell time t_d of 1 s, it was found that nm_s = 2,07, so that with n = 20, one has m_s = 0,1035. Also, $m_s \ln t_p + \ln C$ = –2,09, so that $\beta^{m_s} = 8{,}085\ \text{GPa}^{nm_s} \cdot \text{s}^{m_s} \cdot \text{km}$.

More common is the case in which there is an initial proof test at manufacture. If the second proof test stress is significantly above the first, then Equation (10) can still be used.

In Reference [12], the proof test stress level at manufacture was not stated. A minimum sample length of 10 km or 20 km was used, and each sample was subjected to a different one of five proof test stress levels between 1 GPa and 4 GPa. The proof test speed was reduced to minimize breakage during the start-up acceleration period, so the dwell time t_d was normalized to 1 s using n = 23. The failure probabilities F per meter were calculated for each stress and plotted to fit the straight line of the form

$$\ln\left(\frac{1}{1-F}\right) = M \ln \sigma_p + \ln K \tag{11}$$

With another "ln" on the left (apparently missing), this is equivalent to Equation (101) for static fatigue (ignoring the initial proof-testing) if

$$M \equiv nm_s \text{ and } K \equiv \left(\frac{t_d}{\beta}\right)^{m_s} \tag{12}$$

From this it was determined that M = 1,69, so we find m_s = 0,0735, and K = 0,000418, so that $\beta^{m_s} = 2{,}392\ \text{GPa}^{nm_s} \cdot \text{s}^{m_s} \cdot \text{km}$.

6.4.3 Dynamic fatigue

6.4.3.1 Overview

This is a form of dynamic fatigue testing with censoring, as mentioned in 9.3.3, and with more details on the apparatus given in Reference [5].

6.4.3.2 Data acquisition of dynamic fatigue

A specimen is a single gauge length L_0 of fibre. (A recommended gauge length L_0 is longer than 1 m; for example, 10 m to 20 m.) A sample is a group of specimens from a given population of fibres.

Each specimen is loaded to a failure stress σ_f, or, with censoring, to a (non-failing) maximum stress σ_{max} (for example, 2,4 GPa, about 3,2 % strain from Equation (44)). The recommended strain rate $\dot{\sigma}_a$ is fast (for example, greater than 200 %/min, about 2,6 GPa/s, from Equation (43)). The sample size should be large enough to provide an adequate representation of the second Weibull mode (for example, so that 1 km of the total specimens fail).

The following data are recorded:

– the total number of specimens tested: N, whether or not failure occurred;
– the failure stress values of those specimens that failed: σ_{fi} in GPa. Here i is the rank order, sorted by increasing failure stress.
– the stress rate (converted from strain rate): $\dot{\sigma}_a$ in GPa/s.
– the gauge length of the specimens: L_0 in km.

A Weibull plot in the form of Figure 1 may also be presented (without the curve fittings). The points are measurements from about 0,8 GPa to 2,4 GPa, for an acrylate-coated fused silica fibre with a cladding diameter of 125 μm.

6.4.3.3 Calculation of Weibull parameters

Here the data of the measurement is analysed. According to Equation (86), the Weibull cumulative probability ordinate scale is of the form

$$\ln\left[\ln\left(\frac{1}{1-F}\right)\right],$$

where $F = 1 – P$ is the cumulative failure probability.

Hence compute

$$w_i = \ln\left[-\ln\left(1-\frac{i}{N+1}\right)\right] \tag{13}$$

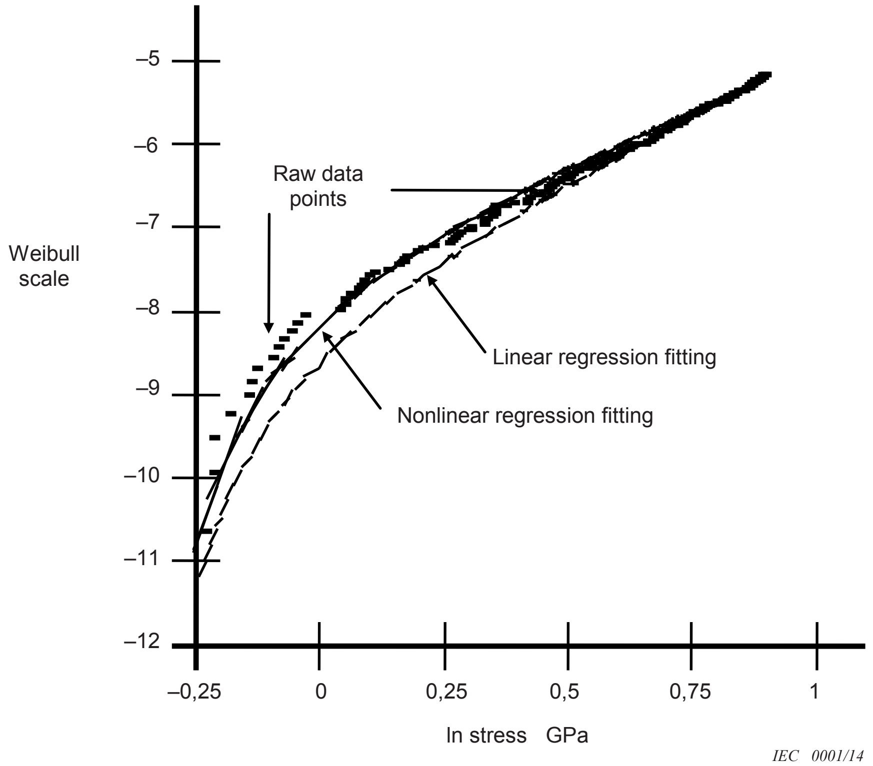

Figure 1 – Weibull dynamic fatigue plot near the proof test stress level

Exponentiate this and use a rearranged form of an approximation (175) of Equation (138)

$$\exp w_i = \frac{\sigma_{fi}^{m_d} L_0}{\left[\dot{\sigma}_a (n+1)\beta\right]^{\frac{m_d}{n+1}}} \times \left\{ \left[1 + \frac{\dot{\sigma}_a (n+1)\sigma_p^n t_p}{\sigma_{fi}^{n+1}}\right]^{\frac{m_d}{n+1}} - \left[\frac{\dot{\sigma}_a (n+1)\sigma_p^n t_p}{\sigma_{fi}^{n+1}}\right]^{\frac{m_d}{n+1}} \right\} \tag{14}$$

Here the length L becomes the testing gauge length L_0.

Two fittings are used on this equation.

a) Linear regression fitting

For large failure stresses, the term in Equation (14) that is enclosed in curled brackets { } approaches one. The equation approaches the "linear" form of the usual Equations (108) and (110) without proof-testing

$$w_i = A + m_d \ln \sigma_{fi} \tag{15}$$

where

$$\ln \beta = \frac{n+1}{m_d}\left(\ln L_0 - A\right) - \ln\left[(n+1)\dot{\sigma}_a\right] \tag{16}$$

Hence for failure stress greater than some selected value, find m_d and A such that the least squares error of w_i is minimized.

This procedure produces the linear regression fitting in Figure 1. Clearly, it would be better to have a closer fit at the left side of this data set, where the values are closer to the applications of interest.

b) Non-linear regression fitting

This uses lower-stress data, where the curvature is apparent. Given a value of m_d, a value of β is computed for each failure stress, and a value from the middle of the data of interest produces a curve that goes through that area. The result produces a sum of squared errors for the entire curve, and m_d is varied to minimize the sum. The steps are indicated below.

- Define a range of data in which the fitting is to be forced. Here it is constructed using ln σ_{fi} values between 0 and 0,5.
- Select a value of m_d.
- Compute ln β_i for each failure stress in the defined region using Equation (14).
- Set ln β equal to the median of the computed ln β_i values.
- Compute $wout_i$ using Equation (14) and the above value of β.
- Compute the squared errors $(w_i - wout_i)^2$, and then compute the sum of squared errors.
- Vary m_d as in the second step, and repeat the remaining steps to minimize the sum.

The procedure produces the non-linear regression fitting in Figure 1.

6.5 Measured numerical values

In this subclause, experimental values resulting from the measurements of 6.4.3 are obtained. They will be used in the calculations of Clause 7.

In 6.3.2, the composite proof test parameter is $\sigma_p^n t_p = 8{,}8849 \times 10^{-5}$ GPa^n·s, with a nominal proof-stress of σ_p = 0,69 GPa (ln σ_p = –0,37 in Figure 1). From 6.3.4 n = 20 is obtained, and in 6.4.3 the stress rate is $\dot{\sigma}_a$ = 4,59477 GPa/s for a gauge length L_0 = 20 m. The non-linear fitting gives the values m_d = 2,359 and ln β = 25,499. Note that β has the unit $\text{GPa}^n \cdot \text{s} \cdot \text{km}^{\frac{n+1}{m_\text{d}}}$.

The static value will also be needed in the following subclause (see Equation (114)):

$$m_s = \frac{m_d}{n+1} \tag{17}$$

which according to the above subclause equals 0,11233. Note too that β now has the unit $\text{GPa}^n \cdot \text{s} \cdot \text{km}^{\frac{1}{m_s}}$ and that β^{m_s} = 17,538 $\text{GPa}^{nm_s} \cdot \text{s}^{m_s} \cdot \text{km}$.

The two values are in reasonable agreement with those of 6.4.2.

7 Examples of numerical calculations

7.1 Overview

The numerical values experimentally obtained in 5.5 are used in the calculations below. The results will be conservative since the explicit B-value is neglected; lower failure rates and longer lifetimes would be obtained if this value were included. (The degree of improvement increases as B increases.) The results of the calculations can be quite sensitive to the choice of parameter values. These values are related to each other, and a change in one parameter will affect the values of other parameters. Ideally, the parameter values should be obtained on the basis of experimentation.

If the failure probability $F = 1 - P$ is 10^{-3} or less (generally the region of practical interest), the term $\ln \frac{1}{P}$ in the formulae below may be replaced by F to an accuracy of 0,5 % or better, but this has not been done in the numerical results given here. See Equation (160)

$$t_f(\text{sec}) = 31\,557\,600\ t_y(\text{yr}) \tag{18}$$

7.2 Failure rate calculations

Compute the failure rates λ that would occur at various static stress levels σ_a as a function of service time t_y in years.

7.2.1 FIT rate formulae

The instantaneous failure rate in FIT is (see Equation (178)):

$$\lambda_i\left(t_f\right) = 3{,}6 \times 10^{12}\, m_s L \left(\frac{\sigma_a^n}{\beta}\right)^{m_s} \left[t_f + t_p \left(\frac{\sigma_p}{\sigma_a}\right)^n\right]^{m_s - 1} \tag{19}$$

The averaged failure rate in FIT is [Equation (179)]

$$\lambda_a(t_f) = \frac{3{,}6 \times 10^{12}}{t_f} \left\langle 1 - \exp\left\{\left[\left(t_p \sigma_p^n\right)^{m_s} - \left(t_f \sigma_a^n + t_p \sigma_p^n\right)^{m_s}\right] \frac{L}{\beta^{m_s}}\right\}\right\rangle \tag{20}$$

NOTE Instantaneous failure rate λ_i in equation (19) is proportional to effective fibre length L. From Equation (20) of average failure rate λ_a, failure probability F is expressed as $\lambda_a\ t_f/(3{,}6 \times 10^{12})$, and F increases from zero and asymptotically approaches to 1 as L increases from zero to infinite. Normally the interest of discussion is a region where $F << 1$ holds, λ_a can be considered approximately proportional to L.

7.2.2 Long lengths in tension

Use several applied stresses, as a fraction of the nominal proof test stress, in the above equations for a fibre length L = 1 km. As a function of time out to 50 years, these give the instantaneous and averaged failure rate plots of Figures 2 and 3, respectively. The corresponding values are given in Table 2. (Zero time is avoided because of the singularity shown there of the averaged failure rate.)

Two points are worth noting. First, all the failure rates are almost constant over time, especially at the lower stresses. This indicates an almost linear increase in total cumulative failures with time. Secondly, and because of this, there is little practical difference in the values between the instantaneous and averaged failure rates.

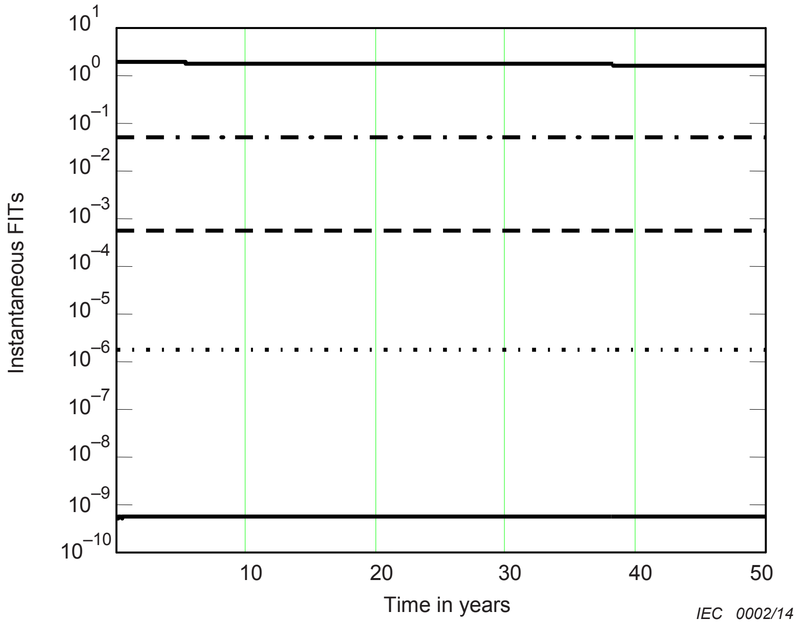

Figure 2 – Instantaneous FIT rates of 1 km fibre versus time for applied stress/proof test stress percentages (bottom to top): 10 %, 15 %, 20 %, 25 %, 30 %

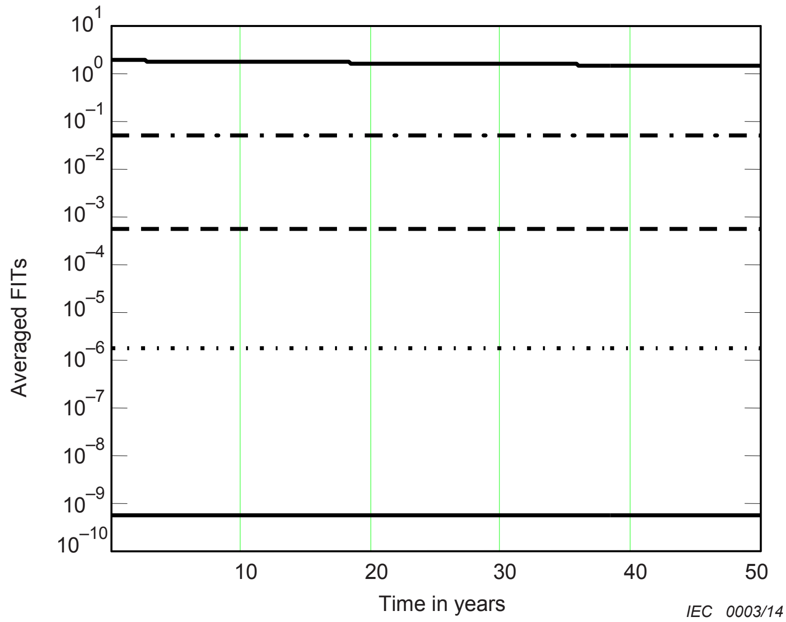

Figure 3 – Averaged FIT rates of 1 km fibre versus time for applied stress/proof test stress percentages (bottom to top): 10 %, 15 %, 20 %, 25 %, 30 %

Table 2 –FIT rates of 1 km fibre in Figures 2 and 3 at various times

Applied stress as a % of proof test stress	Instantaneous FIT						Averaged FIT					
	1 year	10 years	20 years	30 years	40 years	50 years	1 year	10 years	20 years	30 years	40 years	50 years
10	5,45 × 10^{-10}	5,45 × 10^{-10}	5,45 × 10^{-10}	5,45 × 10^{-10}	5,45 × 10^{-10}	5,45 × 10^{-10}	5,45 × 10^{-10}	5,45 × 10^{-10}	5,45 × 10^{-10}	5,45 × 10^{-10}	5,45 × 10^{-10}	5,45 × 10^{-10}
15	1,81 × 10^{-6}	1,81 × 10^{-6}	1,81 × 10^{-6}	1,81 × 10^{-6}	1,81 × 10^{-6}	1,81 × 10^{-6}	1,81 × 10^{-6}	1,81 × 10^{-6}	1,81 × 10^{-6}	1,81 × 10^{-6}	1,81 × 10^{-6}	1,81 × 10^{-6}
20	5,71 × 10^{-4}	5,71 × 10^{-4}	5,71 × 10^{-4}	5,71 × 10^{-4}	5,71 × 10^{-4}	5,71 × 10^{-4}	5,71 × 10^{-4}	5,71 × 10^{-4}	5,71 × 10^{-4}	5,71 × 10^{-4}	5,71 × 10^{-4}	5,71 × 10^{-4}
25	4,95 × 10^{-2}	4,95 × 10^{-2}	4,95 × 10^{-2}	4,93 × 10^{-2}	4,92 × 10^{-2}	4,91 × 10^{-2}	4,95 × 10^{-2}	4,95 × 10^{-2}	4,94 × 10^{-2}	4,94 × 10^{-2}	4,94 × 10^{-2}	4,93 × 10^{-2}
30	1,89 × 10^{0}	1,78 × 10^{0}	1,68 × 10^{0}	1,59 × 10^{0}	1,51 × 10^{0}	1,44 × 10^{0}	1,89 × 10^{0}	1,84 × 10^{0}	1,78 × 10^{0}	1,73 × 10^{0}	1,69 × 10^{0}	1,64 × 10^{0}

7.2.3 Short lengths in uniform bending

From Equations (97) and (98), reduce the actual bend length L_B by the bend-length factor

$$\frac{L}{L_B} = \frac{0{,}4}{\sqrt{nm_s}} \tag{21}$$

which equals 0,266 86 here. From the non-linear Equation (94), the maximum applied stress at the outside fibre surface under bend is

$$\sigma_a(D) = \frac{70{,}33}{8D}\left(1 + \frac{9}{32D}\right) \tag{22}$$

where D is the bend diameter in millimetres. Use several bend diameters in the equations of 7.2.1 for a bent fibre length of 1 m. As a function of time out to 50 years, these give the instantaneous and averaged failure rate plots of Figures 4 and 5, respectively. The corresponding values are given in Table 3.

The "% of proof test stress" number is the percent that the maximum stress (at the outside of the bend) is of the 0,69 GPa proof test stress. Compared with the tensile case of the previous subclause, the constancy of the failure rate with time no longer holds at these higher stresses, especially at shorter times. Also, more significant differences between the instantaneous and averaged values appear, especially at shorter times and tighter bends.

Finally, Table 4 gives results when the non-linear term is not included in Equation (22). As expected, the failure rates are smaller, since the applied stress is slightly underestimated. Moreover, the percentage deviation error from the more correct values of Table 3 increases as the bend diameter decreases and stress increases.

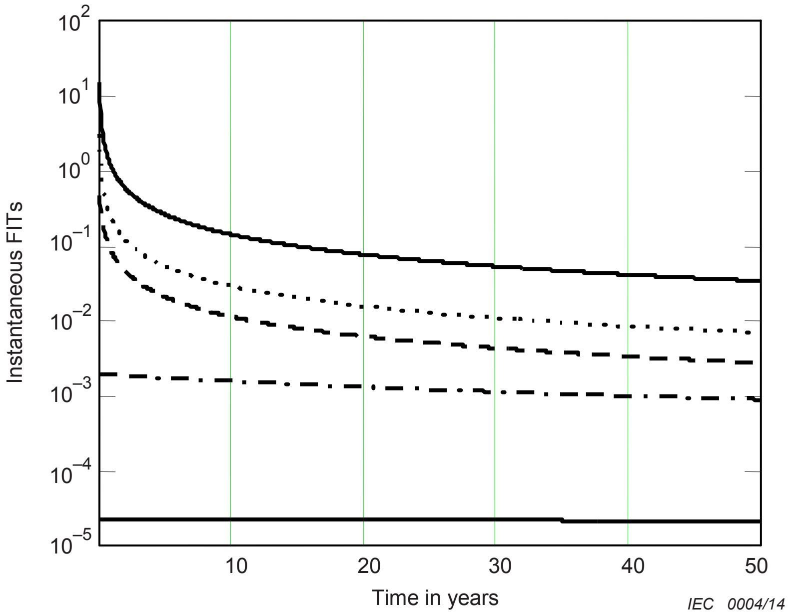

Figure 4 – Instantaneous FIT rates of bent fibre with 1 m effective length versus time

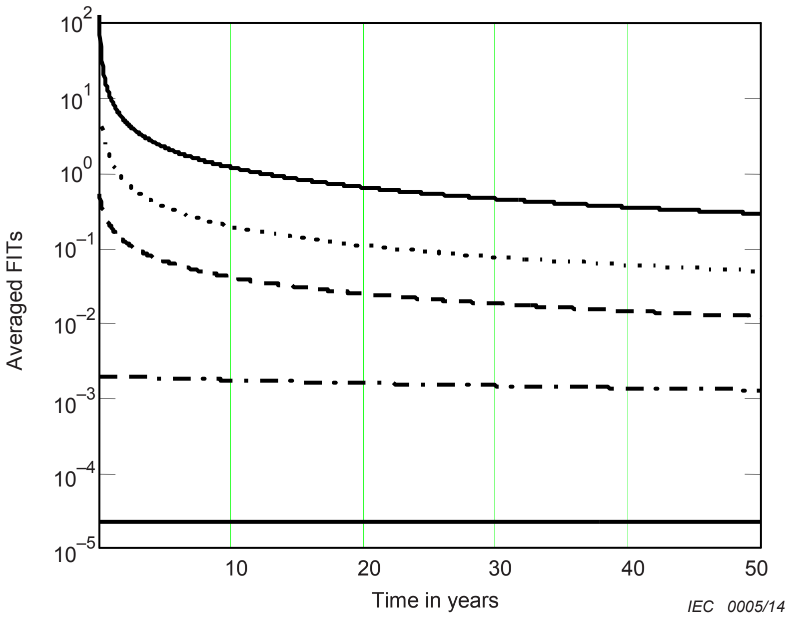

Figure 5 – Averaged FIT rates of bent fibre with 1 m effective length versus time for bend diameters (top to bottom): 10 mm, 20 mm, 30 mm, 40 mm, 50 mm

Table 3 – FIT rates of 1 metre effective length bent fibre in Figures 4 and 5 at various times

Bend diameter (mm), % of proof test stress	Instantaneous FIT in bend						Averaged FIT in bend					
	1 year	10 years	20 years	30 years	40 years	50 years	1 year	10 years	20 years	30 years	40 years	50 years
10, 131,0	$1,08 \times 10^{0}$	$1,40 \times 10^{-1}$	$7,57 \times 10^{-2}$	$5,28 \times 10^{-2}$	$4,09 \times 10^{-2}$	$3,35 \times 10^{-2}$	$9,01 \times 10^{0}$	$1,19 \times 10^{-1}$	$6,43 \times 10^{-1}$	$4,50 \times 10^{-1}$	$3,49 \times 10^{-1}$	$2,86 \times 10^{-1}$
20, 64,6	$2,21 \times 10^{-1}$	$2,86 \times 10^{-2}$	$1,55 \times 10^{-2}$	$1,08 \times 10^{-2}$	$8,35 \times 10^{-3}$	$6,85 \times 10^{-3}$	$1,36 \times 10^{0}$	$1,94 \times 10^{-1}$	$1,07 \times 10^{-1}$	$7,57 \times 10^{-2}$	$5,92 \times 10^{-2}$	$4,88 \times 10^{-2}$
30, 42,9	$8,03 \times 10^{-2}$	$1,13 \times 10^{-2}$	$6,12 \times 10^{-3}$	$4,28 \times 10^{-3}$	$3,33 \times 10^{-3}$	$2,72 \times 10^{-3}$	$1,83 \times 10^{-1}$	$4,06 \times 10^{-2}$	$2,44 \times 10^{-2}$	$1,79 \times 10^{-2}$	$1,44 \times 10^{-2}$	$1,21 \times 10^{-2}$
40, 32,1	$1,88 \times 10^{-3}$	$1,55 \times 10^{-3}$	$1,30 \times 10^{-3}$	$1,12 \times 10^{-3}$	$9,87 \times 10^{-4}$	$8,84 \times 10^{-4}$	$1,91 \times 10^{-3}$	$1,73 \times 10^{-3}$	$1,57 \times 10^{-3}$	$1,45 \times 10^{-3}$	$1,35 \times 10^{-3}$	$1,27 \times 10^{-3}$
50, 25,6	$2,17 \times 10^{-5}$	$2,16 \times 10^{-5}$	$2,15 \times 10^{-5}$	$2,15 \times 10^{-5}$	$2,14 \times 10^{-5}$	$2,14 \times 10^{-5}$	$2,17 \times 10^{-5}$	$2,16 \times 10^{-5}$	$2,16 \times 10^{-5}$	$2,16 \times 10^{-5}$	$2,15 \times 10^{-5}$	$2,15 \times 10^{-5}$

Table 4 – FIT rates of Table 3 neglecting stress versus strain non-linearity

Bend diameter (mm), % of proof test stress	Instantaneous FIT in bend						Averaged FIT in bend					
	1 year	10 years	20 years	30 years	40 years	50 years	1 year	10 years	20 years	30 years	40 years	50 years
10, 127,4	$1,02 \times 10^{0}$	$1,32 \times 10^{-1}$	$7,11 \times 10^{-2}$	$4,96 \times 10^{-2}$	$3,84 \times 10^{-2}$	$3,15 \times 10^{-2}$	$8,43 \times 10^{0}$	$1,11 \times 10^{-1}$	$6,02 \times 10^{-1}$	$4,21 \times 10^{-1}$	$3,27 \times 10^{-1}$	$2,68 \times 10^{-1}$
20, 63,7	$2,14 \times 10^{-1}$	$2,77 \times 10^{-2}$	$1,50 \times 10^{-2}$	$1,03 \times 10^{-2}$	$8,10 \times 10^{-3}$	$6,64 \times 10^{-3}$	$1,30 \times 10^{0}$	$1,86 \times 10^{-1}$	$1,03 \times 10^{-1}$	$7,28 \times 10^{-2}$	$5,69 \times 10^{-2}$	$4,70 \times 10^{-2}$
30, 42,5	$7,73 \times 10^{-2}$	$1,10 \times 10^{-2}$	$5,99 \times 10^{-3}$	$4,19 \times 10^{-3}$	$3,25 \times 10^{-3}$	$2,66 \times 10^{-3}$	$1,68 \times 10^{-1}$	$3,85 \times 10^{-2}$	$2,32 \times 10^{-2}$	$1,71 \times 10^{-2}$	$1,38 \times 10^{-2}$	$1,16 \times 10^{-2}$
40, 31,9	$1,64 \times 10^{-3}$	$1,38 \times 10^{-3}$	$1,18 \times 10^{-3}$	$1,03 \times 10^{-3}$	$9,15 \times 10^{-4}$	$8,25 \times 10^{-4}$	$1,66 \times 10^{-3}$	$1,52 \times 10^{-3}$	$1,40 \times 10^{-3}$	$1,30 \times 10^{-3}$	$1,22 \times 10^{-3}$	$1,15 \times 10^{-3}$
50, 25,5	$1,94 \times 10^{-5}$	$1,93 \times 10^{-5}$	$1,93 \times 10^{-5}$	$1,92 \times 10^{-5}$	$1,92 \times 10^{-5}$	$1,91 \times 10^{-5}$	$1,94 \times 10^{-5}$	$1,93 \times 10^{-5}$	$1,93 \times 10^{-5}$	$1,93 \times 10^{-5}$	$1,93 \times 10^{-5}$	$1,92 \times 10^{-5}$

7.3 Lifetime calculations

Compute the lifetimes that would occur at various static stress levels σ_a as a function of failure probability F.

7.3.1 Lifetime formulae

The lifetime is (see Equation (177))

$$t_f = \left\{ \left[\frac{\beta^{m_s}}{L} \ln \frac{1}{P} + \left(\sigma_p^n t_p \right)^{m_s} \right]^{\frac{1}{m_s}} - \sigma_p^n t_p \right\} \sigma_a^{-n} \qquad (23)$$

7.3.2 Long lengths in tension

Use several applied stresses, as a fraction of the nominal proof test stress σ_p = 0,69 GPa, in the above equation for a fibre length L = 1 km. As a function of failure probability, this gives the lifetime plots of Figure 6. The corresponding values are given in Table 5.

For this example, it appears that an applied stress that is 30 % of the proof test stress is unacceptable at any failure probability level, whereas the 10 % and 15 % values are always acceptable.

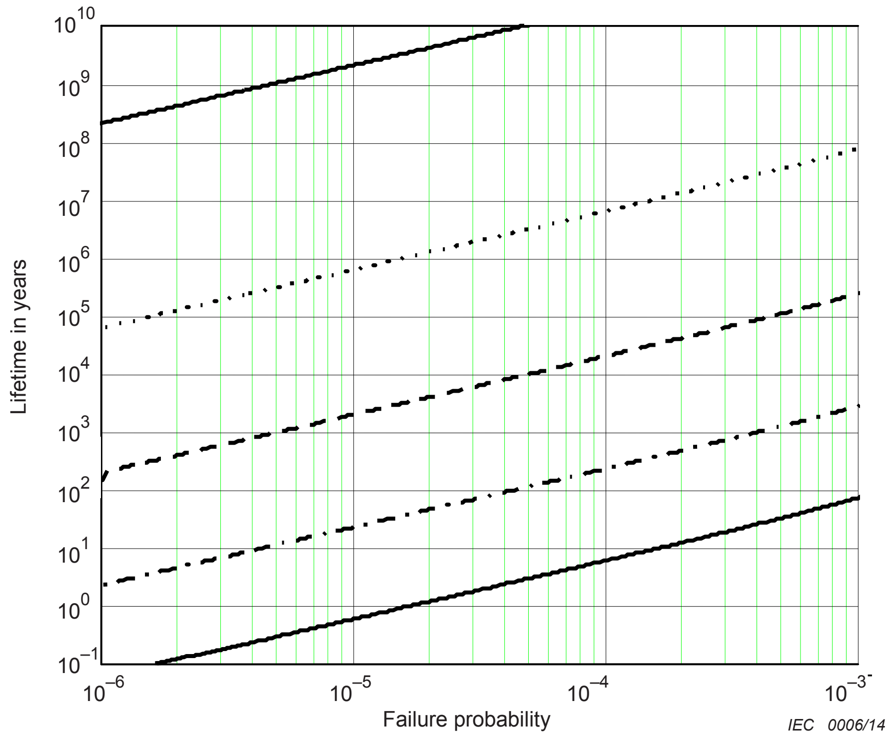

Figure 6 – 1 km lifetime versus failure probability for applied stress/proof test stress percentages (top to bottom): 10 %, 15 %, 20 %, 25 %, 30 %

Table 5 – 1 km lifetimes in years of Figure 6 for various failure probabilities

Applied stress as a % of proof test stress	Failure probability			
	10^{-3}	10^{-4}	10^{-5}	10^{-6}
10	$2,56 \times 10^{11}$	$2,14 \times 10^{10}$	$2,10 \times 10^{9}$	$2,10 \times 10^{8}$
15	$7,70 \times 10^{7}$	$6,43 \times 10^{6}$	$6,31 \times 10^{5}$	$6,30 \times 10^{4}$
20	$2,44 \times 10^{5}$	$2,04 \times 10^{4}$	$2,00 \times 10^{3}$	$2,00 \times 10^{2}$
25	$2,82 \times 10^{3}$	$2,35 \times 10^{2}$	$2,31 \times 10^{1}$	$2,30 \times 10^{0}$
30	$7,35 \times 10^{1}$	$6,13 \times 10^{0}$	$6,02 \times 10^{-1}$	$6,01 \times 10^{-2}$

7.3.3 Short lengths in uniform bending

Calculating failure probability for bent fibre can be accomplished using the length under bend. Use Equation (21) for the bend-length factor and Equation (22) for the maximum applied stress at the outside fibre surface under bend described in this subclause or using the numerical approach described in the bend with tension described in the next subclause. Both methods produce similar results for large diameter bends (greater than 15 mm). For the length under bend estimation use several bend diameters in Equation (177) for a bent fibre length of 1 m. As a function of failure probability, this gives the lifetime plots of Figure 7. The corresponding values are given in Table 6.

Compared with the long length in tension of the previous part, at these higher stresses, there is a greater and non-linear variation in the lifetime with failure probability. It appears that the 30 mm, 40 mm, and 50 mm bends are acceptable at almost all the failure probabilities.

Finally, Table 7 gives results when the non-linear term is not included in Equation (22). As expected, the lifetimes are larger, since the applied stress is slightly underestimated. Moreover, the percentage deviation error from the more correct values of Table 6 increases as the bend diameter decreases and stress increases.

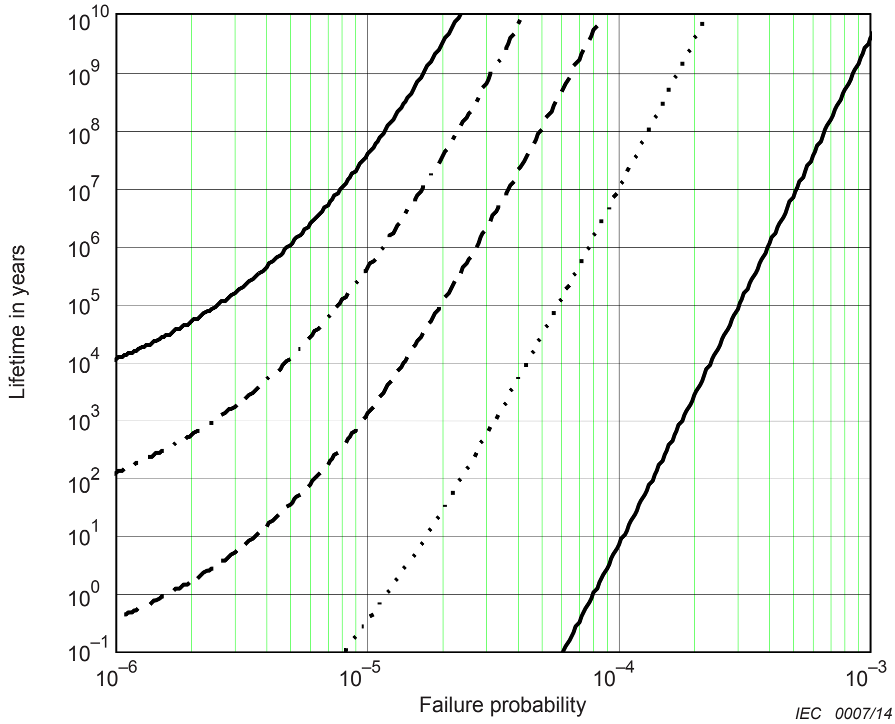

Figure 7 – Lifetimes of bent fibre with 1 m effective length versus failure probability for bend diameters (bottom-right to top-left): 10 mm, 20 mm, 30 mm, 40 mm, 50 mm

Table 6 – Lifetimes of bent fibre with 1 m effective length in years of Figure 7 for various failure probabilities

Bend diameter mm	% of proof test stress	Failure probability			
		10^{-3}	10^{-4}	10^{-5}	10^{-6}
10	131,0	$3,83 \times 10^{9}$	$7,23 \times 10^{0}$	$2,57 \times 10^{-7}$	$7,69 \times 10^{11}$
20	64,6	$5,28 \times 10^{15}$	$9,99 \times 10^{6}$	$3,54 \times 10^{-1}$	$1,06 \times 10^{-4}$
30	42,9	$1,93 \times 10^{19}$	$3,64 \times 10^{10}$	$1,29 \times 10^{3}$	$3,87 \times 10^{-1}$
40	32,1	$6,37 \times 10^{21}$	$1,20 \times 10^{13}$	$4,27 \times 10^{5}$	$1,28 \times 10^{2}$
50	25,6	$5,68 \times 10^{23}$	$1,07 \times 10^{15}$	$3,81 \times 10^{7}$	$1,14 \times 10^{4}$

Table 7 – Lifetimes in years of Table 6 neglecting stress versus strain non-linearity

Bend diameter mm	% of proof test stress	Failure probability			
		10^{-3}	10^{-4}	10^{-5}	10^{-6}
10	127,4	$6{,}66 \times 10^{9}$	$1{,}26 \times 10^{1}$	$4{,}47 \times 10^{-7}$	$1{,}34 \times 10^{-10}$
20	63,7	$6{,}99 \times 10^{15}$	$1{,}32 \times 10^{7}$	$4{,}69 \times 10^{-1}$	$1{,}40 \times 10^{-4}$
30	42,5	$2{,}32 \times 10^{19}$	$4{,}39 \times 10^{10}$	$1{,}56 \times 10^{3}$	$4{,}67 \times 10^{-1}$
40	31,9	$7{,}33 \times 10^{22}$	$1{,}38 \times 10^{13}$	$4{,}91 \times 10^{5}$	$1{,}47 \times 10^{2}$
50	25,5	$6{,}35 \times 10^{23}$	$1{,}20 \times 10^{15}$	$4{,}26 \times 10^{7}$	$1{,}28 \times 10^{4}$

7.3.4 Short lengths with uniform bending and tension

Optical cables are traditionally designed to separate bending forces from axial tensions. This assumption is not valid for drop cables used in building applications as described in Reference [22]. These small diameter low fibre count cables may be routed through existing construction with practices similar to copper and may be subject to bends and tension simultaneously. Under these demanding conditions, the strain from all sources should be taken into account to accurately predict mechanical lifetime at the bend.

The resulting failure probability when bends and tension are present can be calculated using the strip calculation. The difference in the calculation is that instead of using Equation (21) for effective length, the calculation is done for a number of surface strips, each of which has a different static stress. The probability of surviving the load period is calculated for each strip. The sum of these probabilities is the probability that all strips will survive. One minus probability of overall survival yields probability of failure.

Equation (21) is derived from assumptions that include a uniform Weibull slope and which do not include the proof test. Doing the strip calculation allows taking the actual distribution into account. It also allows the introduction of tensile load to bending.

The strip calculation

Calculate the maximum bend stress, σ_b, as a function of bend diameter, D, as

$$\sigma_b(D) = \frac{70{,}33}{8D}\left(1 + \frac{9}{32D}\right) \tag{24}$$

Define the number of strips as n_s and designate the strips with index, i, ranging from 0 to n_{s1}. It has been found that i should be at least 20 to get reasonable results. Define $\theta = i2\pi/n_s$. A tensile load stress, σ_t, in addition to bend stress is also allowed. Calculate the stress for each strip, σ_i, as:

$$\sigma_i = \max\left[\sigma_b \cos(\theta_i) + \sigma_t, 0\right] \tag{25}$$

Calculate the natural logarithm of the probability of survival for each strip, ln(P_i), as:

$$\ln(P_i) = \left[\left(t_p\sigma_p^n\right)^{m_s} - \left(t_f\sigma_i^n + t_p\sigma_p^n\right)^{m_s}\right]\frac{L/n_s}{\beta^{m_s}} \tag{26}$$

Where L (km) is the length of fibre under bend and tension. Calculate the probability of failure, F, as:

$$F = 1 - \exp\left[\sum_i \ln(P_i)\right] \quad (27)$$

Calculate average FIT as:

$$FIT = \frac{3.6 \times 10^{12}}{t_f} F \quad (28)$$

This calculation can be used with no tension and will provide reasonable agreement with the failure rates described in the previous section. The tensile load option allows one to calculate the failure rate for the combination of bend and tension. Table 8 shows the result for L = 1 m when 30 % proof test is added to each radii for a 30 year case.

Table 8 – Calculated results in case of bend plus 30 % of proof test tension for 30 years

Bend diameter mm	Failure probability of 1 m fibre	Average FIT of 1 m fibre	Average FIT/turn
10	$1{,}87 \times 10^{-4}$	$7{,}10 \times 10^{-1}$	$2{,}23 \times 10^{-2}$
15	$9{,}00 \times 10^{-5}$	$3{,}42 \times 10^{-1}$	$1{,}61 \times 10^{-2}$
20	$5{,}53 \times 10^{-5}$	$2{,}10 \times 10^{-1}$	$1{,}32 \times 10^{-2}$
30	$2{,}90 \times 10^{-5}$	$1{,}10 \times 10^{-1}$	$1{,}04 \times 10^{-2}$
40	$1{,}88 \times 10^{-5}$	$7{,}15 \times 10^{-2}$	$8{,}99 \times 10^{-3}$

Except for the purpose of comparison, it would probably be better to calculate failure probability in a configuration similar to deployment such as 1 ¼ or ½ turn. For 10 mm diameter full turn, this works out to around 6×10^{-6}.

8 Fibre weakening and failure

NOTE Individual cracks in the glass are considered first. Their statistical nature is treated in Clause 11.

8.1 Crack growth and weakening

The theory of fibre strength, as shown in Reference [1], follows the theory of brittle materials. It assumes that very small imperfections or cracks are distributed along the length of glass. For a silica-based fibre, the critical cracks are mostly at the surface where they are vulnerable to attack and weakening by moisture, dust, chemicals, etc. For silica-based optical fibres, polymer coatings around the glass or a hermetic film (for example, amorphous carbon film, plus coating) on the glass are intended to slow these effects.

The stress intensity factor at a crack tip is defined as a function of time t to be

$$K_I(t) = Y\sigma(t)a^{\frac{1}{2}}(t) \quad (29)$$

assumed to hold in any environment of interest.

Here

Y is a dimensionless crack geometry shape parameter (assumed to be constant),

σ is the positive applied stress, and

a is the flaw "depth", that is, the flaw size normal to the direction of applied stress. The distribution of crack sizes is statistical, as will be discussed in Clause 11.

In the ideal inert environmental condition of low temperature (for example, liquid N_2), or zero humidity, or high vacuum, cracks will grow only at the critical velocity and will then fracture. For a crack of constant size, the applied-stress intensity factor in Equation (29) varies proportionally to the time-varying stress applied to the crack. The factor has a maximum value K_{Ic}, called the "critical stress intensity factor or fracture toughness". This occurs when the applied stress increases to its allowable maximum given by the inert strength S of the crack (typically above 15 GPa for a short length of pristine fibre), so at this instant the time-varying Equation (29) becomes

$$K_{Ic} = YSa^{\frac{1}{2}} \tag{30}$$

At this point, catastrophic failure occurs. Because of the required environment, inert strength is difficult to measure, and this has led to non-unique values obtained experimentally. We typically will use the term "strength" rather than "inert strength" to mean the limiting value of failure stress that would be measured for "instant fracture" under static or dynamic fatigue. (This is described mathematically in 9.4.3.) The value may have a dependence on the environment in which this measurement would occur.

For the fibre in a non-inert or active (ambient or hostile) environment, such as at higher temperatures and with humidity, water, or chemical species, any applied stress will cause crack growth to occur. This is called stress corrosion, since hydrolysis of silica bonds occurs. The values of the shape parameter Y and the fracture toughness K_{Ic} are uncertain to at least 10 %, but are assumed constant for that type of crack over a wide range of environments.

Then Equation (30) establishes a one-to-one relationship between the increasing crack size in the active environment with the decreasing strength that could be approximately measured in an inert environment, or for instant fracture. Numerically, with assumed values of $Y \approx 1{,}24$ for an elliptical crack under tension and $K_{Ic} \approx 0{,}8$ MPa·m$^{1/2}$, Equation (30) is

$$a(\mu\text{m}) = 0{,}42[S(\text{GPa})]^{-2} \tag{31}$$

A strength of 0,7 GPa in the proof test stress region corresponds to a crack size of about 0,88 μm. In the high-strength region, 7 GPa corresponds to a crack size of only 8,8 nm. The latter is not much larger than the tetrahedral structural units of the glass, so the concept of a "crack" may be more useful as a model rather than being physically significant in this region.

In a non-inert environment, the rate of crack growth or crack growth velocity V is assumed to be related to the stress intensity factor by the empirical equation

$$\frac{da}{dt} = V(t) = AK_I^n(t) = V_c\left[\frac{K_I(t)}{K_{Ic}}\right]^n \tag{32}$$

This contains the critical crack growth velocity at the instant of failure

$$V_c = AK_{Ic}^n \tag{33}$$

Here, A is a material scaling parameter that depends on the environment through the critical crack growth velocity. For example, V_c is expected to increase as the partial pressure of water increases. The dimensionless exponent n is the crack's stress corrosion susceptibility parameter, or n-value for short. The power law relationship of Equation (32) holds in the linear region I of the $\log \dot{a}$ versus $\log K_I$ curve, where n is the slope of the line. This may have little physical basis, but is justified by the results it produces in approximating experimental results. Both n and A (which includes a dependence upon n) depend upon the particular environment.

In the treatment below, "strength" rather than "crack size" will be referred to, although they are interchangeable via Equations (30) and (31). To calculate how a crack weakens (loses strength) as stress is applied, one substitutes the stress intensity factor of Equation (33) into Equation (32) for crack growth and eliminates crack size via Equation (30). This gives the strength variation with applied stress

$$\frac{dS^{n-2}(t)}{dt} = -\frac{\sigma^n(t)}{B} \tag{34}$$

Here one defines the crack's strength preservation parameter or B-value (for short)

$$B^{-1} = \left(\frac{n}{2}-1\right) A Y^2 K_{Ic}^{n-2} = \left(\frac{n}{2}-1\right) V_c \left(\frac{Y}{K_{Ic}}\right)^2 \tag{35}$$

The parameter depends upon the environment through the earlier-defined parameters in this equation. It will not be necessary later in this standard to individually know them all to be able to calculate B. However, to measure it is difficult (see 13.4), and quoted values may range from 10^{-8} to 1 $\text{GPa}^2 \cdot \text{s}$.

Equation (34) can be integrated so that if the fibre is subjected to a stress history $\sigma(t)$, a particular crack at an initial time 0 and of an initial strength $S(0)$ will weaken to a strength $S(t)$ given in

$$S^{n-2}(t) = S^{n-2}(0) - \frac{1}{B}\int_0^t \sigma^n(\bar{t})d\bar{t} \quad \text{with} \quad \sigma(t) < S(t) \tag{36}$$

or

$$\frac{S(t)}{S(0)} = \left\{1 - \frac{S^2(0)}{B}\int_0^t \left[\frac{\sigma(\bar{t})}{S(0)}\right]^n d\bar{t}\right\}^{\frac{1}{n-2}} \tag{37}$$

The flaw does not break so long as its remaining strength exceeds the applied stress. The last term on the right side accounts for the dynamic characteristics of the applied stress and the fibre's response to it via the environmentally dependent parameters n and B. Note that in Equations (36) and (37) crack weakening (and growth) occurs so long as n exceeds 2, though common values may range from 15 to 30 for typical fibres to over a hundred for hermetic fibres. Moreover, a particular applied stress history will have a smaller weakening effect on a fibre having a higher value of B (in keeping with its name).

8.2 Crack fracture

In the previous subclause, the crack grew and weakened but did not break. With fracture, the critical failure condition of Equation (30) occurs just when the final strength in Equations (36) and (37) equals the applied stress at the instant of failure t_f, that is

$$t = t_f \text{ and } S(t_f) = \sigma(t_f) \tag{38}$$

(In another interpretation the crack size has grown to the critical value given by Equations (30) and (31).) Using this condition and the strength degradation Equations (36) and (37), one obtains the general lifetime equation

$$\sigma^{n-2}(t_f) = S^{n-2}(0) - \frac{1}{B}\int_0^{t_f} \sigma^n(t)dt \tag{39}$$

or

$$\frac{S(0)}{\sigma(t_f)} = \left\{1 + \frac{\sigma^2(t_f)}{B}\int_0^{t_f}\left[\frac{\sigma(t)}{\sigma(t_f)}\right]^n dt\right\}^{\frac{1}{n-2}} \tag{40}$$

The ratio under the integral sign becomes unity at fracture. Either form of this equation implicitly gives the lifetime t_f for any stress history $\sigma(t)$ in a given fixed environment.

Further simplification is useful for those cases in which the left side in Equation (39) is negligible, that is the fracture stress is somewhat less than the initial strength. For example, that fracture stress term is negligible (less than ~1 % of the other two terms) when

$$\sigma(t_f) \le 0{,}01^{\frac{1}{n-2}} S(0) \tag{41}$$

For the examples n = 15 and 30, this holds if the applied fracture stress is less than 70 % and 85 % of the initial strength, respectively. Hence if sufficient crack weakening (crack growth) has occurred, the general lifetime equation of Equation (39) is simply

$$\int_0^{t_f} \sigma^n(t)dt = BS^{n-2}(0) \tag{42}$$

An advantage of this form is that now B and $S^{n-2}(0)$ do not need to be known separately but only in a product. (Also, it results in the linearized plots below of Equation (46) for static fatigue and Equation (47) for dynamic fatigue, so this approximation is often used in the literature.)

8.3 Features of the general results

- Crack weakening in Equations (36) and (37) and crack failure in Equations (39) and (40) depend on the magnitude of the applied stress and upon the duration of the stress application, as well as the crack parameters n and B.
- These general results can be applied to many different practical problems concerning fibre weakening or failure due to applied stress. Some of these problems will be treated below; they include proof-testing, which is intended to be non-destructive, the destructive tests of static fatigue and dynamic fatigue, and predicting service lifetime or failure rate.
- Equations (40) and (41) for crack weakening may be applied repeatedly, for example, to the proof-testing during manufacture, to destructive fatigue testing, to a dormant shipping period of almost zero stress, to the cabling process, and to field deployment. The strength decrease during each period (from beginning to end) may thus be calculated.
- All results assume that the strength decreases with time as a function of the applied stress alone. For a fixed environment, the fatigue parameters are assumed to remain unchanged with time. This is a limitation because they have been observed to change with temperature and humidity, and no mapping functions of these parameters versus environment have been agreed upon.
- Strength can change in harsh environments, even when no stress is applied; this is called zero-stress ageing. In the intrinsic region, the small-flaw strength often decreases;

whereas in the proof test region, the strength of the larger flaws sometimes increases. Experiments may sometimes mix the two phenomena, and, if the effects are not separated, the analysis of results can produce incorrect estimates of the fatigue parameters.

– For reliability estimates, careful engineering judgement is required concerning the stress history and the environmental conditions the fibre experienced before installation, the strength distribution, the fatigue parameters, the ageing characteristics, and the stresses and environments expected in the field application.

8.4 Stress and strain

Instead of using stress, one may speak of the associated fractional increase in length, the strain ε. The two are related in References [2], [3] by the quadratic relationship

$$\sigma(\varepsilon) = E_0(1+c\varepsilon)\varepsilon \tag{43}$$

Here E_0 is the zero-strain Young's modulus which has values of 70,3 GPa to 73,8 GPa. The non-linearity term c has ranged from 3 to 3,3 for axial strain; we will use the former here. Due to asymmetric stress distributions, the value changes in other geometries are discussed in Reference [4] and briefly in 11.3. In this technical report, stress will be used rather than strain. Inverting Equation (43) gives strain in terms of stress

$$\varepsilon(\sigma) = \frac{\left(E_0^2 + 4E_0 c\sigma\right)^{\frac{1}{2}} - E_0}{2E_0 c} \tag{44}$$

A stress of 0,7 GPa, typically used as a proof test stress, corresponds to a strain of 0,92 % to 0,97 %.

A perfectly circular glass fibre is assumed with a diameter of 125 μm and the coating contribution to load is ignored. Then 1 GPa stress is equivalent to a force of 12,272 N or a load of 1 251,4 g.

9 Fatigue testing

9.1 Overview

The means by which the crack parameters mentioned in 8 may be measured are then examined. One method is by fatigue testing applied destructively to numerous fibre specimens of a fixed gauge length. This allows for the measurement of n and the product BS^{n-2}. There are two types of fatigue testing, and the subscripts *s* and *d* refer to parameters measured under static and dynamic conditions, respectively.

9.2 Static fatigue

In static fatigue, a fibre specimen is subjected to a constant applied stress σ_a until the weakest crack of initial strength S breaks at an observed failure time t_f. This stress history is shown schematically in Figure 8. From Equations (39) and (40) the failure time is

$$t_f(\sigma_a) = B_s \sigma_a^{-n_s}\left(S^{n_s-2} - \sigma_a^{n_s-2}\right) \tag{45}$$

If the stress-to-strength ratio is sufficiently small, such as in Equation (41), or if the approximate lifetime in Equation (42) is used, then this has the reduced form

$$t_f(\sigma_a) \approx B_s S^{n_s-2} \sigma_a^{-n_s} = t_f(1) \sigma_a^{-n_s} \quad (46)$$

This has the unit-stress "intercept" value

$$t_f(1) = B_s S^{n_s-2} \quad (47)$$

which depends upon the units used. Note that this intercept does not have the dimension of time.

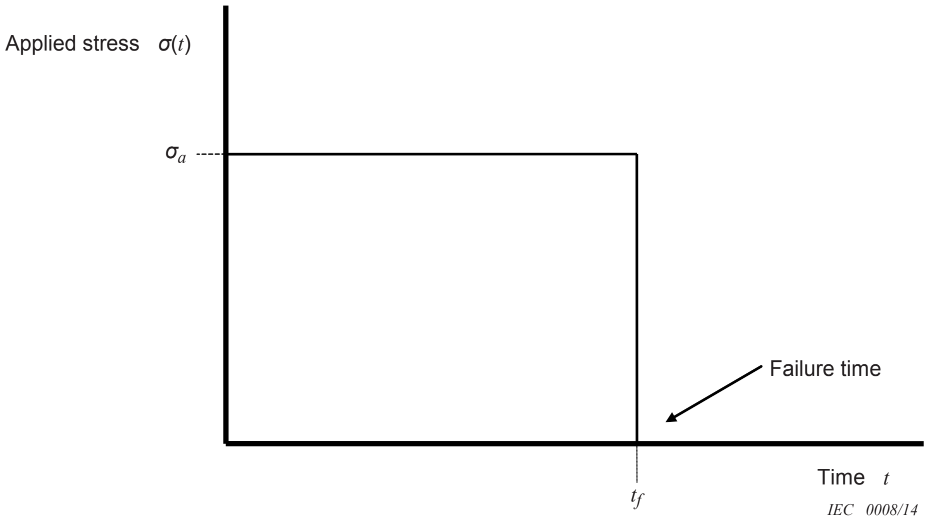

Figure 8 – Static fatigue – Applied stress versus time for a particular applied stress

In static fatigue testing, different stresses are applied to different sets of specimens. From Equation (46), a double-logarithmic plot of failure times versus applied stresses gives

$$\lg t_f(\sigma_a) \approx \lg t_f(1) - n_s \lg \sigma_a \quad (48)$$

The data should lead to a best-fit straight line with a negative slope of $-n_s$ and a vertical intercept of $\lg t_f(1)$. (This value will depend on the units used, and may require a straight-line extrapolation beyond the data points.) This data is shown schematically in Figure 9. According to Equation (45), non-linearities are expected for large applied stress or weak flaws. As discussed in 9.4.4, this can lead to errors in measuring n_s.

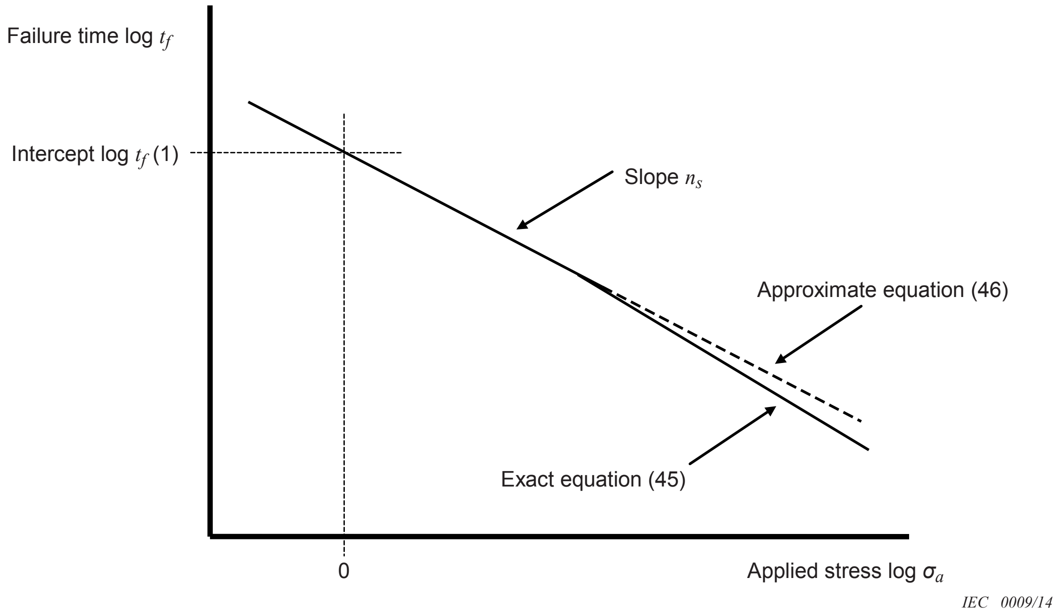

Figure 9 – Static fatigue – Schematic data of failure time versus applied stress

9.3 Dynamic fatigue

9.3.1 Overview

This test is performed in either of two ways. In one, the stress is applied until the fibre breaks. In the other, the stress is applied to a maximum value or until the fibre breaks, whichever occurs first.

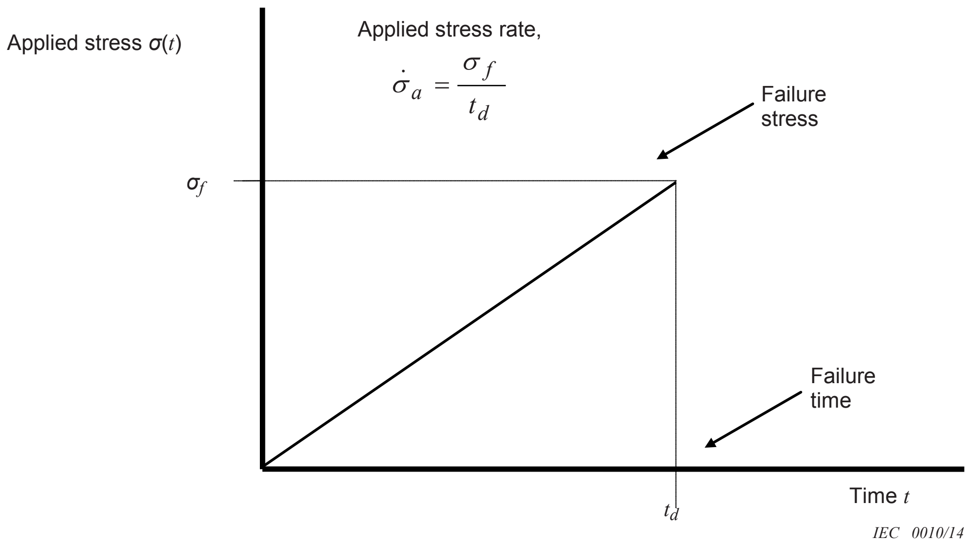

Figure 10 – Dynamic fatigue – Applied stress versus time for a particular applied stress rate

9.3.2 Fatigue to breakage

In the more common dynamic fatigue a fibre specimen is subjected to a constant applied stress rate $\dot{\sigma}_a$ until the weakest crack of initial strength S breaks at an observed failure time t_d, or dynamic fatigue failure stress

$$\sigma_f = \dot{\sigma}_a t_d \tag{49}$$

This stress history is shown schematically in Figure 10. (Do not confuse t_d with proof-testing dwell time defined in 10.2.) From Equations (39) and (40), the failure stress is

$$\sigma_f(\dot{\sigma}_a) = \left[(n_d + 1)B_d \dot{\sigma}_a \left(S^{n_d - 2} - \sigma_f^{n_d - 2}\right)\right]^{\frac{1}{n_d + 1}} \tag{50}$$

If the stress-to-strength ratio is sufficiently small according to Equation (41), or if the approximate lifetime of Equation (42) is used, then this has the reduced form

$$\sigma_f(\dot{\sigma}_a) \approx \left[(n_d + 1)B_d \dot{\sigma}_a S^{n_d - 2}\right]^{\frac{1}{n_d + 1}} = \sigma_f(1)\dot{\sigma}_a^{\frac{1}{n_d + 1}} \tag{51}$$

This has the unit-stress-rate "intercept" value

$$\sigma_f(1) = \left[(n_d + 1)B_d S^{n_d - 2}\right]^{\frac{1}{n_d + 1}} \tag{52}$$

which depends upon the units used. Note that this intercept does not have the dimension of stress. One can also work with t_d versus σ_f or $\dot{\sigma}_a$, but these formats are less common.

In dynamic fatigue testing, different stress rates are applied to different sets of specimens. From Equation (51), a double-logarithmic plot of failure stresses versus stress rates gives

$$\lg \sigma_f(\dot{\sigma}_a) \approx \lg \sigma_f(1) + \frac{\lg \dot{\sigma}_a}{n_d + 1} \tag{53}$$

The data should lead to a best-fit straight line with a slope of $(n_d + 1)^{-1}$ and a vertical intercept of $\lg\sigma_f(1)$. This value will depend on the units used and may require a straight-line extrapolation beyond the data points. This data is shown schematically in Figure 11. According to Equation (50), non-linearities are expected for large failure stresses or weak flaws. As discussed in 9.4.4, this can lead to errors in measuring n_d.

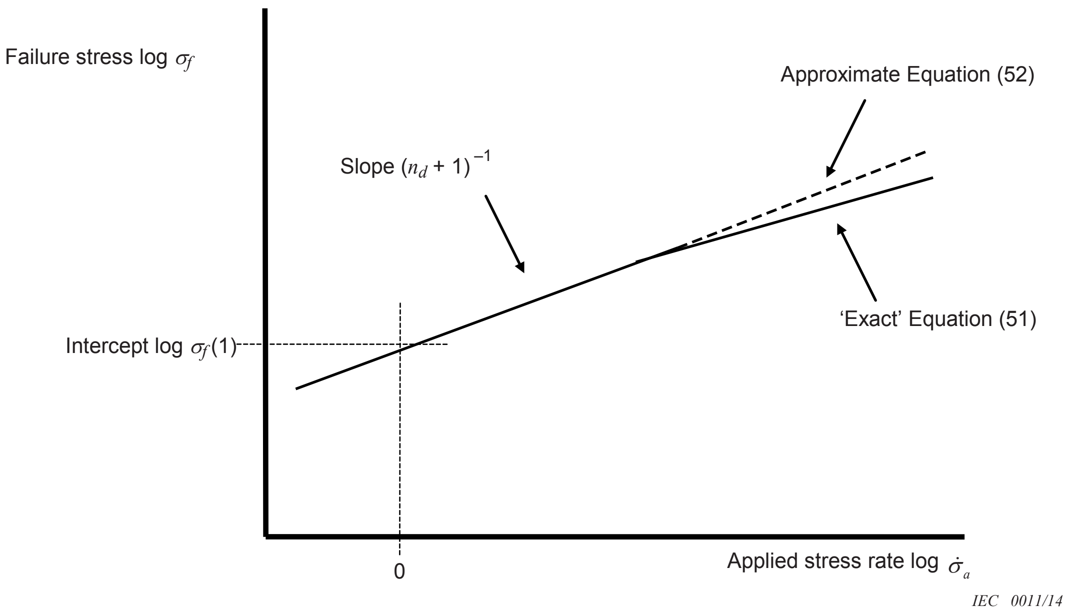

Figure 11 – Dynamic fatigue – Schematic data of failure time versus applied stress rate

9.3.3 Fatigue to a maximum stress

For long-term reliability prediction, it is useful to obtain data in the low-strength low-fracture-probability portion of the Weibull distribution discussed in 11.2.2, 11.5, and 11.8. Except for fibre deployments that involve very high stresses, very tight bends, or rather high allowable failure probabilities, it is these cracks that are more important. One method of characterizing these cracks is dynamic fatigue testing with censoring.

According to Reference [5], the method differs in several ways from the usual dynamic fatigue testing. The gauge length is longer, and more samples are used. Both these factors mean that a very long length of fibre is tested. Only one high strain rate is applied, and the resulting applied stress is limited to a maximum value σ_{max} within the lower mode of the Weibull strength distribution. The stress history is similar to that of Figure 10 with a constant stress rate, but with the highest stress being either σ_f with breakage or σ_{max} without breakage. The latter is more common, and this means that a smaller fraction of fibre from a longer sampled length is broken.

More details of the measurements and calculations are given in 9.4.2 and 9.4.3.

9.4 Comparisons of static and dynamic fatigue

9.4.1 Intercepts and parameters obtained

The parameters n and B obtained statically or dynamically should, in principle, be equal for the same environment. With a few exceptions for the n-value, we will drop the subscripts s and d from this point forward. Then Equations (47) and (52) relate the intercepts as

$$BS^{n-2} = t_f(1) = \frac{\sigma_f^{n+1}(1)}{n+1} \qquad (54)$$

9.4.2 Time duration

Static fatigue experiments are usually carried out over longer periods of time (days to months) and may be conducted in a hostile environment (elevated temperature, humidity, and possible chemical species). Dynamic fatigue is usually carried out over shorter periods of time (seconds to hours), often (but not always) in an inert or ambient environment. For many applications, it is necessary to assess the strength distribution in the neighbourhood of the proof test stress, usually by dynamic fatigue testing.

Solving Equation (46) for $t_f(1)$ and Equation (51) for $\sigma_f(1)$, and using Equation (54) gives

$$\sigma_a^n t_f = \frac{\sigma_f^{n+1}}{(n+1)\dot{\sigma}_a} \tag{55}$$

This suggests that if the static applied stress is taken equivalent to the dynamic fatigue failure stress, then as in Reference [6]

$$t_f = \frac{\sigma_f}{(n+1)\dot{\sigma}_a} = \frac{t_d}{n+1} \tag{56}$$

where Equation (49) has been used. This means that an "effective" static fatigue failure time results from dividing the dynamic fatigue failure time by $n + 1$.

In an extended approach, two flaws of different initial inert strengths S_1, S_2 prior to static and dynamic fatigue are equivalent, if from the "exact" static lifetime Equation (45)

$$\left(\frac{S_1}{\sigma_a}\right)^{n-2} = 1 + \frac{\sigma_a^2 t_f}{B} \tag{57}$$

and from the "exact" dynamic fatigue failure stress Equation (50)

$$\left(\frac{S_2}{\sigma_f}\right)^{n-2} = 1 + \frac{\sigma_f^3}{(n+1)B\dot{\sigma}_a} \tag{58}$$

Equating the left sides leaves

$$t_f = \frac{\sigma_f^3}{\sigma_a^2 (n+1)\dot{\sigma}_a} \tag{59}$$

Equation (55) was applied to dynamic and static fatigue results taken at several laboratories on the same fibre measured in various deployment geometries in Reference [6]. When the non-linear corrections of Equation (43) and the area corrections of 11.3 were incorporated, the static and dynamic n-values in a static fatigue type plot fell on the same line. But the slope of the line varied to give n-values ranging from 17 at high stress/short time to 40 at low stress/long time.

9.4.3 Dynamic and inert strengths

From Equations (49) and (50), the ratio of inert strength to failure stress (or "dynamic strength") is

$$\frac{S}{\sigma_f} = \left[1 + \frac{\sigma_f^3}{(n+1)B\dot{\sigma}_a}\right]^{\frac{1}{n-2}} = \left[1 + \frac{\sigma_f^2 t_d}{(n+1)B}\right]^{\frac{1}{n-2}} \tag{60}$$

which approaches unity as the stress rate (or B-value) increases. This explains why high stress rates are sometimes used to experimentally estimate inert strength.

9.4.4 Plot non-linearities

In static fatigue, the failure time decreases as the constant applied stress increases, according to Equation (45). The applied stress approaches the "inert" strength as the failure time vanishes. For the plot of ln t_f versus ln σ_a according to Equation (48), the more exact Equation (45) leads to a

$$\text{static fatigue logarithmic slope} = -\frac{n_s - 2\left(\dfrac{\sigma_a}{S}\right)^{n_s-2}}{1-\left(\dfrac{\sigma_a}{S}\right)^{n_s-2}} \tag{61}$$

As the applied stress increases, the plot of Figure 9 will curve downwards such that the absolute value of the slope increases from n_s to higher values, so that the apparent n_s is larger.

In dynamic fatigue, the failure stress or dynamic strength increases with stress rate, according to Equation (50). For example, if n_d = 15 and 30, increasing the stress rate by a factor of 1 000 (which is often done in dynamic fatigue testing) increases the dynamic strength by 54 % and 25 %, respectively. Moreover, the proportionality factors relating the two strengths depend upon the environment (through B and n). These factors impact the manner in which vendors or users can specify "strength".

For the plot of ln σ_f versus ln $\dot{\sigma}_a$ according to Equation (53), the more exact Equation (50) leads to a

$$\text{dynamic fatigue logarithmic slope} = \frac{1}{(n_d+1)\left[1+\dfrac{(n_d-2)B_d\dot{\sigma}_a}{\sigma_f^3}\right]} \tag{62}$$

As the applied stress rate increases, the plot of Figure 11 will somewhat flatten such that the value of the slope decreases from $(n_d + 1)^{-1}$ to smaller values, so that the apparent n_d is larger.

Because n increases with longer duration tests, as discussed in the last paragraph of 9.4.2, increased steepness of the static fatigue curve at very low stresses and decreased steepness of the dynamic fatigue curve at very low stress rates are observed. In these cases, the static and dynamic n-values converge.

9.4.5 Environments

The dependence of crack parameters on environment is under continuing investigation. An understanding of the effects of temperature, humidity, and other environments on crack growth would permit the "mapping" from one environment to another. It would also permit the use of shorter-term "accelerated ageing" in harsh environments to predict reliability for longer-term service in more benign environments.

In a truly inert environment, the failure stress is independent of the stress rate. This is equivalent to putting either n or B equal to infinity in Equations (51) through (53).

10 Proof-testing

10.1 Overview

This clause shows how proof-testing reduces "infant mortalities" and determines important reliability features.

NOTE This clause references the B-value, and this is done for theoretical completeness only. There are as yet no agreed methods for measuring B, and Clause 10 develops theoretical results for the special case in which B can be neglected.

10.2 The proof test cycle

Proof-testing requires that a nominally constant proof test stress σ_p be applied sequentially along the full length of the fibre. Unlike fatigue testing, it is not performed necessarily to failure, although, as discussed in 11.6, a break rate (failures per unit length) N_p is statistically expected. This is done during fibre manufacturing, on-line as part of the fibre drawing and coating process, or off-line as part of the testing process.

The stress history of proof test stressing, shown schematically in Figure 12, is

– stress loading from near-zero to the proof test stress, during a loading time t_l,
– constant proof test stress σ_p during a dwell time t_d (symbol not to be confused with the dynamic fatigue failure time defined in 9.3),
– stress unloading from the proof test stress back down to near-zero, during an unloading time t_u.

Consider a fibre proof-tested at a fibre speed s. The loading/unloading time across a quarter turn of a wheel of diameter D is then $t_{l,u} = \frac{\pi D}{4s}$. The fibre dwell-length is st_d.

As shown in Figure 12 and References [7] to [10], it is assumed that the load and unload processes are essentially linear. The load and unload portions are similar to dynamic fatigue, and the dwell is somewhat similar to static fatigue. The differences are that the maximum applied stress (the proof test stress) is limited and that breakage does not necessarily occur. Since this topic is particularly complex, equivalence to equations in the references (often with varying approaches and notations) are given in the development below.

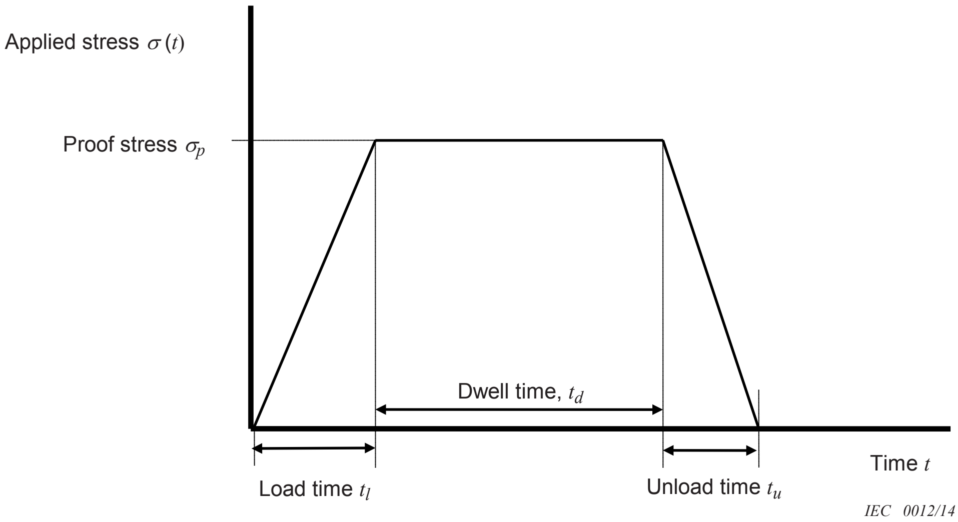

Figure 12 – Proof-testing – Applied stress versus time

10.3 Crack weakening during proof-testing

Equations (36) and (37) for weakening show that for a crack that does not break, its initial "inert" strength S before proof-testing has reduced to an "inert" strength S_p after proof-testing, where

$$S_p^{n-2} = S^{n-2} - \frac{\sigma_p^n t_p}{B} \tag{63}$$

Here the effective proof test time is given by

$$t_p = t_d + \frac{t_l + t_u}{n+1} \tag{64}$$

This is equivalent to Equation (7) of Reference [7]. In this equation, the loading time t_l and unloading time t_u in the fraction contribute little to the effective proof test time. As an example, if $n \geq 20$, and neither the loading time nor unloading time exceeds 10 % of the dwell time, the fraction in Equation (64) constitutes less than 1 % of the effective proof test time. This shows that the dwell time t_d should be kept small so as to minimize the fatigue of the surviving cracks.

A crack that has an initial strength (before proof-testing) not exceeding the proof test stress will weaken and break during loading. A stronger crack will weaken and will break during the dwell if its strength degrades to the proof test stress. If it survives the dwell, it has a strength $S_u(0)$ just before unloading at least equal to the proof test stress; however, further weakening occurs during unloading. During a time t into the unloading, the applied stress is

$$\sigma_u(t) = \sigma_p\left(1 - \frac{t}{t_u}\right) = \sigma_p - \dot{\sigma}_u t \tag{65}$$

where the (positive) unloading rate is

$$\dot{\sigma}_u = \frac{\sigma_p}{t_u} \tag{66}$$

Using Equations (65) and (66) in Equations (36) and (37), the monotonically decreasing crack strength during unloading is obtained as

$$S_u^{n-2}(t) = S_u^{n-2}(0) - \frac{\sigma_p^n t_u}{(n+1)B}\left[1-\left(1-\frac{t}{t_u}\right)^{n+1}\right] \tag{67}$$

This is equivalent to Equation (7) of Reference [8].

10.4 Minimum strength after proof-testing

10.4.1 Overview

For the weakest crack just surviving the proof test, the minimum final strength from Equation (63) equals the minimum strength after unloading from Equation (67), so that

$$S_{p\min} = S_{u\min}(t_u) \tag{68}$$

There are two situations by which this strength is determined, depending upon whether the unloading process is "fast" or "slow." This relates to the dimensionless quantity

$$\alpha = \frac{\sigma_p^2 t_u}{(n-2)B} = \frac{\sigma_p^3}{(n-2)B\dot{\sigma}_u} \tag{69}$$

explicitly containing fibre and proof test unloading parameters. As shown below, it is important whether this quantity is larger or smaller than unity.

10.4.2 Fast unloading

Here the weakest crack just before unloading has its strength equal to the proof test stress, that is

$$S_{umin}(0) = \sigma_p \tag{70}$$

During unloading, the decreasing strength from Equation (67) is larger than the rapidly decreasing unload stress of Equation (65), so that fracture does not occur. The rates of decrease for both strength and applied stress just before unloading shall satisfy

$$\left|\frac{dS_u(t)}{dt}\right|_{t=0} \leq \dot{\sigma}_u \tag{71}$$

Applying Equation (66) to Equation (67) and using Equation (69) implies that $\alpha \leq 1$. Then Equations (67) and (70) give the minimum crack strength after proof-testing

$$S_{p\min} = \sigma_p \left[1 - \frac{\sigma_p^2 t_u}{(n+1)B}\right]^{\frac{1}{n-2}} = \sigma_p \left(1 - \frac{n-2}{n+1}\alpha\right)^{\frac{1}{n-2}} \tag{72}$$

for $\alpha \le 1$ or $t_u \le (n-2)\dfrac{B}{\sigma_p^2}$

This is equivalent to Equation (9) of Reference [8]. For fast unloading, $B \ge B_0$.

10.4.3 Slow unloading

Here the weakest crack just before unloading has its strength exceeding the proof test stress, that is

$$S_{u\min}(0) \ge \sigma_p \tag{73}$$

For failure at some time $\hat{t}$ during unloading, the decreasing strength of Equation (67) equals the decreasing unloading strength of Equation (65), that is,

$$S_{u\min}(\hat{t}) = \sigma_u(\hat{t}) = \sigma_{\min} \le \sigma_p \tag{74}$$

where σ_{min} is a minimum value of the failure stress. Then putting Equations (68) and (74) into Equation (67) gives the minimum crack strength after proof-testing

$$S_{p\min} = \sigma_p \left[1 - \frac{\sigma_p^2 t_u}{(n+1)B}\right]^{\frac{1}{n-2}} \tag{75}$$

This is equivalent to Equation (9) of Reference [7]. The unknown minimum failure stress σ_{min} can be determined by noting that at the critical survival time $\hat{t}$, the strength and stress curves are equal but do not quite intersect. They are tangential, so that at that point

$$\left|\frac{dS_u(t)}{dt}\right|_{t=\hat{t}} = \dot{\sigma}_u \tag{76}$$

Equations (76), (67) and (69) leave

$$\sigma_{\min}^3 = (n-2)B\dot{\sigma}_u = \frac{\sigma_p^3}{\alpha} \tag{77}$$

This and Equation (74) imply that $\alpha \ge 1$, and Equation (75) gives

$$S_{p\min} = \left(\frac{3}{n+1}\right)^{\frac{1}{n-2}} \left[(n-2)B\dot{\sigma}_u\right]^{\frac{1}{3}} = \sigma_p \left(\frac{3}{n+1}\right)^{\frac{1}{n-2}} \alpha^{-\frac{1}{3}} \tag{78}$$

for $\alpha \geq 1$ or $t_u \geq (n-2)\dfrac{B}{\sigma_p^2}$

These are equivalent to Equations (10) and (11) of Reference [7], and to Equation (10) of Reference [8]. For slow unloading, $B \leq B_0$.

Note that here the unloading rate is the only proof test (non-crack) parameter determining the minimum surviving strength (which is now independent of the proof test stress itself). Equations (72) and (78) both show the importance of minimizing the unloading time t_u as stated in IEC 60793-1-30.

10.4.4 Boundary condition

At the boundary between the fast-unloading and slow-unloading conditions, α =1. Then Equation (69) gives the transitional B-value.

$$B_0 = \frac{\sigma_p^2 t_u}{n-2} \tag{79}$$

which can also be solved for the unloading time. From Equations (72) and (78), the minimum surviving strength at the boundary is

$$S_{p\min} = \sigma_p \left(\frac{3}{n+1}\right)^{\frac{1}{n-2}} \tag{80}$$

10.5 Varying the proof test stress

One effect of increasing (similar considerations apply for decreasing) the proof test stress is to increase the minimum surviving strength according to Equations (72) and (78). Another is to increase the fibre break rate (or decrease the survival length), as will be shown in Clause 11. This has been used in References [11] and [12] to probe the low-strength distribution over long fibre lengths, and is detailed in 6.4.2.

11 Statistical description of strength by Weibull probability models

11.1 Overview

So far, single cracks with deterministic values of particular parameters have been considered. Now it is assumed that for a particular type of crack most parameters are constant but that strengths are statistically distributed in value.

11.2 Strength statistics in uniform tension

11.2.1 Unimodal probability distribution

A fibre of circular geometry that is uniform along its length is assumed. When simple longitudinal tension is applied to it, there are two degrees of stress uniformity, both along the fibre length and in the fibre cross-part. (Fibre volume or surface area may instead be used as the prime dimension.) Call $N(S)$ the cumulative number of flaws per unit length having an "inert" strength equal to or less than S. If a fibre length L is put under stress, call $P(S, L)$ the cumulative survival probability up to the strength S. (A parallel derivation can be made in terms of the flaw size a.) In this "weakest link" model, the incremental probability that the fibre fails in the strength interval S to $S + dS$ is

$$[1 - P(S + dS, L)] - [1 - P(S, L)] \tag{81}$$

This equals the probability of survival to the failure strength times a quantity proportional to the number of flaws in that strength interval

$$P(S, L)hL[N(S + dS) - N(S)] \tag{82}$$

where h is a proportionality constant. Equating Equations (81) and (82), integrating and using the boundary condition of no flaws of zero strength, leads to the Weibull survival_distribution

$$P(S,L) = e^{-hLN(S)} \tag{83}$$

Usually, the literature speaks in terms of the cumulative failure probability $F = 1 - P$. Here P is used to simplify the notation. Often it is found (or assumed) that

$$N(S) \propto S^m \tag{84}$$

where m is the Weibull parameter for the inert environment.

Using Equations (83) and (84) leaves the cumulative survival probability, as in Reference [13]

$$P(S,L) = \exp\left[-\left(\frac{S}{S_0}\right)^m \frac{L}{L_0}\right] \tag{85}$$

The boundary conditions are such that survival is certain at zero strength or length, and failure is certain at infinite strength or length. Here S_0 is the Weibull strength parameter measured at a "gauge" length L_0, corresponding to a survival probability of e^{-1} or 36,8 %. The "inert" m-value is related to the variance or 'width' of the distribution with respect to strength and determines the variation of strength with fibre length. Furthermore,

$$\ln\ln\frac{1}{P(S,L)} = m\ln\frac{S}{S_0} + \ln\frac{L}{L_0} \tag{86}$$

so that for a fixed length, a scaled cumulative failure probability plot versus inert strength leaves a straight line of slope m. Increasing the length will increase the probability intercept. Proof-testing will distort the distribution, as discussed in 11.6.

The probability distribution function, a continuous "histogram" of the survival population, is

$$p(S,L) = -\frac{\partial P}{\partial S} = \frac{m}{S_0}\frac{L}{L_0}\left(\frac{S}{S_0}\right)^{m-1} P(S,L) \tag{87}$$

This is related to the number of flaws per unit length having an "inert" strength S given by

$$\frac{\partial N}{\partial S} = \frac{p(S,L)}{LP(S,L)} = \frac{m}{S_0 L_0}\left(\frac{S}{S_0}\right)^{m-1} \tag{88}$$

Here Equations (83) through (85) and Equation (87) have been used.

For a given survival probability, the strength can be predicted for another length in terms of the gauge values

$$S(L,P) = S_0\left(L_0, e^{-1}\right)\left(\frac{L_0}{L}\ln\frac{1}{P}\right)^{\frac{1}{m}} \tag{89}$$

Similarly, for a given strength, the survival probabilities of both lengths are related by

$$L_0 \ln P(S, L) = L \ln P(S, L_0) \tag{90}$$

Extrapolation to longer fibre lengths in the above equations is uncertain, since weaker flaws of a "different type" may appear. They will have a different set of values for the Weibull parameters as per the bimodal distribution below.

11.2.2 Bimodal probability distribution

If there are two flaw types, there are two main ways of statistically describing them according to Reference [14]. With concurrent flaw distributions, both flaw types are present in all specimens. This is the case with specimens from one manufacturer. Here, the survival probability distribution is the product of the individual survival probability distributions for each flaw type. With exclusive flaw distributions, a given specimen may contain only one flaw type. An example would be specimens from two manufacturers. In this case, the survival probability distribution is the sum of the individual survival probability distributions for each flaw type. Partially concurrent distributions can also be modelled.

Fibre flaws are likely of the concurrent type so that the Weibull assumption of Equation (85) becomes

$$P(S,L) = \exp\left[-\left(\frac{S}{S_{01}}\right)^{m_1}\frac{L}{L_{01}} - \left(\frac{S}{S_{02}}\right)^{m_2}\frac{L}{L_{02}}\right] \tag{91}$$

Here (m_1, S_{01}) and (m_2, S_{02}) characterize each flaw, while gauge lengths L_{01} and L_{02} provide a weighting factor for the two flaw types. This type of distribution can describe the "knee" found in plotting measured data. The steeper distribution of high-strength breaks is attributable to silica bonding, and this is the region of "intrinsic" flaws. The lower-slope distribution of low-strength "extrinsic" flaws is introduced during the manufacturing process. Proof-testing will generally affect only the latter segment of the population distribution.

Plots with negative curvature can be fit to exclusive or partially concurrent distributions.

11.3 Strength statistics in other geometries

11.3.1 Stress non-uniformity

It is usually assumed that the glass fibre is perfectly circular, with a radius a_f constant with length L (although non-uniformities can be corrected for in principle). The effect of the coating on stress calculation is often neglected or only approximately accounted for. The treatment in the text until now has been for longitudinal tension in which the stress is uniformly applied along the fibre length. Stress then equals the fraction [tension/(πa_f^2)]. With non-uniform stress, the exponent in the survival probability in Equation (85) for unimodal distributions has $S^m L$ replaced by the integral over the sample surface (assuming interior flaws are negligible)

$$I = \int_A S^m(A)dA \tag{92}$$

Two configurations have commonly been treated mathematically, as in References [15] and [16].

11.3.2 Uniform bending

Here, a bend of radius R (with respect to the fibre axis) is applied uniformly along a fibre length L_b, as around a mandrel. The resulting applied stress is uniform along the bent fibre length, but it varies on the fibre surface as

$$\sigma_a(\theta) = \sigma_{max}\sin\theta \tag{93}$$

In the cross-part of the fibre, the angle θ is with the axis perpendicular to the bend plane and passing through the fibre axis. The maximum stress occurs along a line on the outside of the fibre bend and in the plane of the bend. It has the value

$$\sigma_{\max}(R) = E_0\left(1+\frac{9}{4}\frac{a_f}{R}\right)\frac{a_f}{R} \tag{94}$$

using the non-linear effect of Equation (43) with a geometrical correction from Reference [4]. For a fibre with a diameter $2a_f$ = 125 μm, the error in calculating stress while neglecting the non-linear term exceeds 1 % when the bend diameter $2R$ is less than about 28 mm. Also, a maximum stress of 0,7 GPa corresponds to a bend diameter of about 13 mm (depending upon the assumed value of Young's modulus).

The incremental area at the above stress is

$$dA = L_b a_f d\theta \tag{95}$$

Integration according to Equation (92) leaves the Weibull forms similar to Equation (85) and to the later Equations (100), and (107), but with the bend length replaced by the equivalent tensile length

$$L = \frac{L_b}{\pi}\int_0^{\frac{\pi}{2}} \sin^x\theta \, d\,\theta \tag{96}$$

This defines the length in uniform straight tension at the maximum stress σ_{max}, giving the same probability distribution as for the real length under uniform bending. This result applies to the approximate static Weibull distribution of Equation (101) and to the approximate dynamic Weibull distribution of Equation (108). It does not apply to those distributions after proof-testing in Equations (122), (132), and (138).

A better fit for Equation (96) is

$$L \approx 0{,}4\frac{L_b}{\sqrt{x}} \tag{97}$$

a result independent of the bend radius. In this equation there is the factor

$$x = \frac{mn}{n-2} = m_s n = \frac{m_d n}{n+1} \tag{98}$$

using inert, static fatigue, and dynamic fatigue parameters, respectively. The equivalent length is some fraction of the real bend length.

11.3.3 Two-point bending

Here the fibre is bent between parallel flat plates in a "U" fashion. The tension is non-uniform, both in the fibre cross-part and length, and reaches a maximum value at the mid-point of the outside of the bend. Similar to Equation (94) and as in Reference [4], that value is about

$$\sigma_{\text{max}}(D) = 2{,}4 E_0 \left(1 + 0{,}51 \frac{a_f}{D}\right) \frac{a_f}{D} \tag{99}$$

where D is the separation of the fibre axes in the straight portions of the "U". Moreover, the equivalent tensile length decreases as that stress increases, and the analysis becomes very complicated, as in Reference [15]. One calculates a length range of only 10 μm to 30 μm at typical failure strains, but the precise equivalent length is difficult to determine.

Now consider how the fatigue testing of Clause 9, carried out in non-inert active (ambient or hostile) environments, affects the inert Weibull probability distribution introduced in 11.2. Then add the proof-testing of Clause 10, which affects mainly the low-strength extrinsic region of the bimodal distribution. We show how both static and dynamic fatigue testing preserve the linear nature of the distribution, but proof-testing distorts and truncates it.

However, in fatigue testing, the applied stress and the failure stress are usually larger than the proof test stress. This is not so for most practical longer-term service conditions. The Weibull parameters obtained this way apply only to the high-strength segment of a bimodal distribution and cannot be extrapolated to lower failure probability values. To obtain values that apply to the lower-strength segment including the proof test stress region, longer fibre lengths must be tested. An example is given in 9.3.3.

11.4 Weibull analysis for static fatigue before proof-testing

For a particular value of stress σ_a applied to a fibre length L, there is some statistical variation in the measured failure times t_f. The initial strength prior to static fatigue is given by Equation (57), which substituted into the Weibull probability Equation (85) leaves the static survival probability

$$P(t_f) = \exp\left[-\left(\frac{t_f + \dfrac{B}{\sigma_a^2}}{t_0}\right)^{m_s}\right] \tag{100}$$

$$\approx \exp\left[-\left(\frac{t_f}{t_0}\right)^{m_s}\right] \text{when } t_f >> \frac{B}{\sigma_a^2} \tag{101}$$

The usual approximate form in Equation (101) is equivalent to Equation (5) of Reference [17]. Here the static Weibull parameter is related to the "inert" m-value (not usually known) via

$$m_s = \frac{m}{n-2} \tag{102}$$

The Weibull time-scaling parameter is

$$t_0 = \frac{\beta}{L^{\frac{1}{m_s}} \sigma_a^n} \tag{103}$$

where $$\beta = BS_0^{n-2} L_0^{\frac{1}{m_s}} \tag{104}$$

These depend upon several crack and measurement parameters and can be calculated from static fatigue testing on gauge fibre lengths L_0 at several applied stresses according to 9.2.

From any probability value, one can calculate

$$t_0 = \left(t_f + \frac{B}{\sigma_a^2} \right) \left[\ln \frac{1}{P(t_f)} \right]^{\frac{1}{m_s}} \tag{105}$$

A convenient point is the "intercept" for unity failure time; convenient probability values are e^{-1} (36,8 %) or ½ (corresponding to the median lifetime). Furthermore, from Equation (100) one obtains

$$\ln\ln \frac{1}{P(t_f)} = m_s \ln \left[\frac{t_f + \frac{B}{\sigma_a^2}}{t_0} \right] \tag{106}$$

so that a scaled cumulative failure probability plot versus failure time leaves a straight line of slope m_s. This preserves the form of the inert Equation (85) and is shown schematically in Figure 13 for a bimodal distribution.

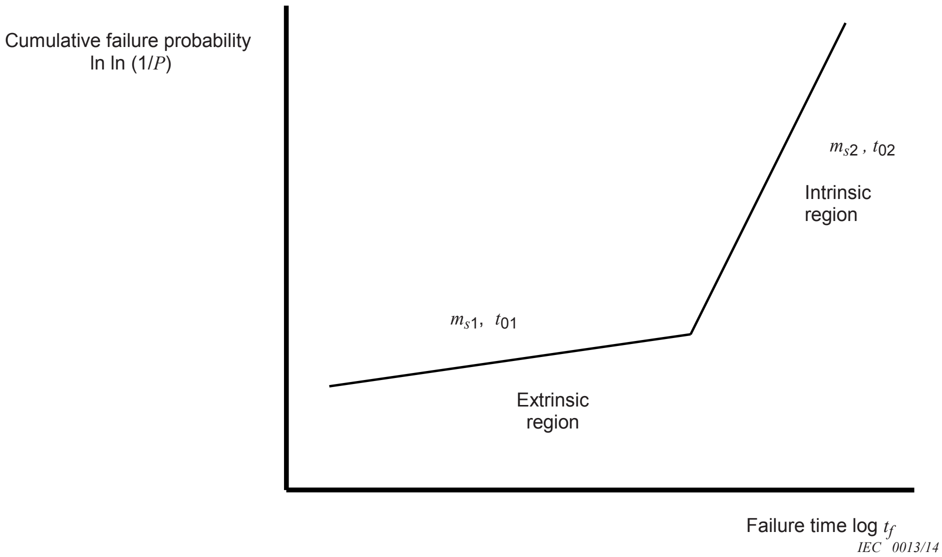

Figure 13 – Static fatigue schematic Weibull plot

11.5 Weibull analysis for dynamic fatigue before proof-testing

For a particular value of stress rate $\dot{\sigma}_a$ applied to a fibre length L, there is some statistical variation in the measured failure stresses σ_f. The initial strength prior to dynamic fatigue is given by Equation (58) which, substituted into the Weibull probability Equation (85), leaves the dynamic fatigue survival probability

$$P(\sigma_f) = \exp\left\langle -\left\{ \frac{\sigma_f}{\sigma_0}\left[1 + \frac{(n+1)B\dot{\sigma}_a}{\sigma_f^3}\right]^{\frac{1}{n+1}} \right\}^{m_d} \right\rangle \tag{107}$$

$$\approx \exp\left[-\left(\frac{\sigma_f}{\sigma_0}\right)^{m_d}\right] \text{when } \sigma_f^3 >> (n+1)B\dot{\sigma}_a \tag{108}$$

The usual approximate form in Equation (108) is equivalent to Equation (6) of Reference [17]. Here the dynamic Weibull parameter is related to the "inert" m-value (not usually known) via

$$m_d = \left(\frac{n+1}{n-2}\right)m \tag{109}$$

The Weibull stress-scaling parameter is

$$\sigma_0 = \frac{[(n+1)\beta\dot{\sigma}_a]^{\frac{1}{n+1}}}{L^{\frac{1}{m_d}}} \tag{110}$$

where $$\beta = BS_0^{n-2} L_0^{\frac{n+1}{m_d}} \tag{111}$$

These depend upon several crack and measurement parameters and can be calculated from dynamic fatigue testing on a fibre length L_0 at several applied stress rates, according to 9.3.

From any probability value, one can calculate

$$\sigma_0 = \sigma_f \left[\ln \frac{1}{P(\sigma_f)} \right]^{-\frac{1}{m_d}} \left[1 + \frac{(n+1)B\dot{\sigma}_a}{\sigma_f^3} \right]^{\frac{1}{n+1}} \tag{112}$$

A convenient point is the "intercept" for unity failure stress; convenient probability values are e^{-1} (36,8 %) or ½ (corresponding to the median failure stress). Furthermore, from Equation (107), one obtains

$$\ln\ln \frac{1}{P(\sigma_f)} = m_d \ln \frac{\sigma_f}{\sigma_0} + \frac{m_d}{n+1} \ln \left[1 + \frac{(n+1)B\dot{\sigma}_a}{\sigma_f^3} \right] \tag{113}$$

so that a scaled cumulative failure probability plot versus failure stress leaves a straight line of slope m_d. This preserves the form of the inert Equation (85) and is shown schematically in Figure 14 for a bimodal distribution.

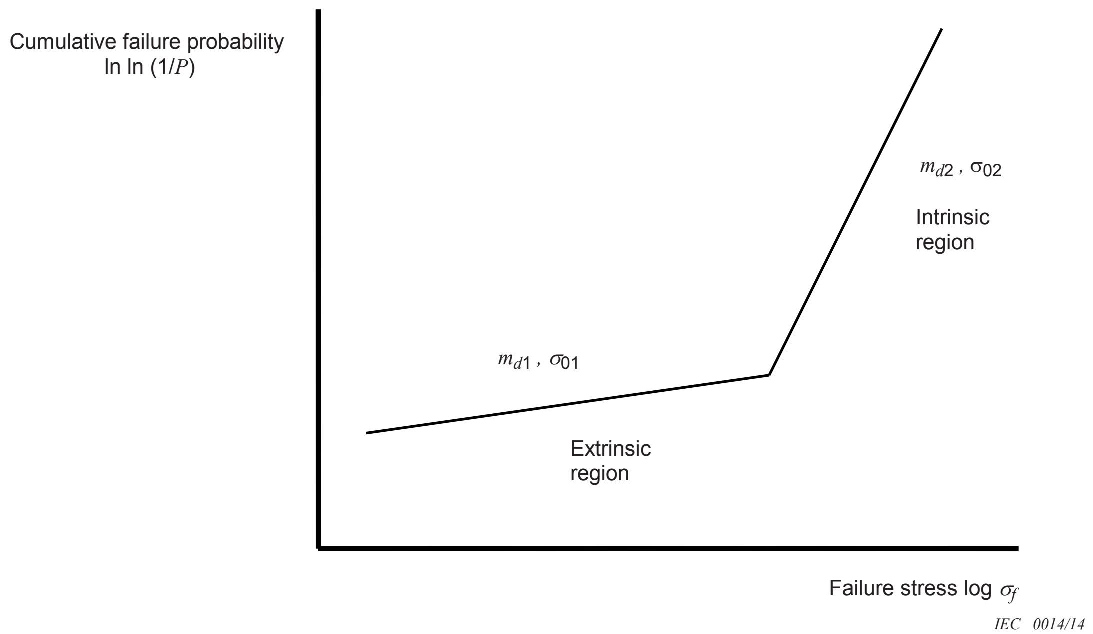

Figure 14 – Dynamic fatigue schematic Weibull plot

From Equations (102) and (109), the static and dynamic Weibull parameters are related by

$$m_d = (n + 1)m_s \tag{114}$$

Then comparing Equations (103) and (110), the static and dynamic Weibull parameters are related by

$$\sigma_0^{n+1} = (n+1)\dot{\sigma}_a \sigma_a^n \; t_0 \qquad (115)$$

This is analogous to the relation of static and dynamic plot intercepts given by Equation (54).

11.6 Weibull distribution after proof-testing

Here it is shown how the "inert" strength distributions of 11.2 are modified by the proof test procedure. Fatigue testing probes fibre survival probability by breaking many samples of limited gauge length. On the other hand, proof-testing is applied to the whole fibre length with the intent of breaking only those cracks with strengths below some specified minimum value. As discussed below, this enhances the survival probability of the remaining usable fibre.

As a function of final strength S_p after proof-testing, the enhanced survival probability P_p equals the survival probability as a function of initial strength S before proof-testing, divided by the survival probability as a function of the minimum initial strength S_{min} at the proof test stress

$$P_p(S_p) = \frac{P(S)}{P(S_{\min})} \qquad (116)$$

Now we use the inert Weibull Equation (85), though the bimodal Equation (91) usually applies. However, in the comparatively weak "extrinsic" flaw region around the proof test level, the first unimodal term there will predominate, and one has

$$\ln \frac{1}{P_p(S_p)} = \left(\frac{S^m - S_{\min}^m}{S_0^m} \right) \frac{L}{L_0} \qquad (117)$$

For simplification, we will suppress the several variables implicit in P_p, and will use $\ln \frac{1}{P_p}$ to eliminate the exponential functions and reduce the number of brackets.

The right side of such an equation is always non-negative, and zero for certain survival P_p = 1. If the failure probability $F_p = 1 - P_p < 10^{-3}$, which is generally the region of practical interest, the term $\ln \frac{1}{P_p}$ may be replaced by F_p to within an accuracy of 0,5 % or better.

The minimum initial strength at the proof test stress level is related to the number of failures per unit length (break rate) during proof-testing, obtained by Equations (84) and (85)

$$N_p = \left(\frac{S_{\min}}{S_0} \right)^m \frac{1}{L_0} \qquad (118)$$

Then Equation (117) becomes, assuming $S >> S_{min}$,

$$\ln \frac{1}{P_p(S_p)} \approx N_p L \left(\frac{S}{S_{\min}} \right)^m \qquad (119)$$

This form is equivalent to Equation (19) of Reference [8]. Taking the mean with respect to length shows that N_p is the mean break rate, ideally a small number. It is convenient to define the mean survival length after proof-testing

$$L_p = \frac{1}{N_p} = \left(\frac{S_0}{S_{\min}}\right)^m L_0 \tag{120}$$

using Equation (118), ideally a large number.

For the above equations, Equation (63) relates strength before proof-testing to strength after proof-testing; it also relates their minimum values as

$$S_{p\min}^{n-2} = S_{\min}^{n-2} - \frac{\sigma_p^n t_p}{B} \tag{121}$$

where the minimum strength for cracks just surviving the proof test stress is given by Equations (72) or (77), depending upon the value of α. By use of Equations (63) and (121), Equations (117) and (119) become the survival probability distribution after proof-testing

$$\ln\frac{1}{P_p(S_p)} = \left\{\left(BS_p^{n-2} + \sigma_p^n t_p\right)^{\frac{m}{n-2}} - \left[\sigma_p^n t_p(1+C)\right]^{\frac{m}{n-2}}\right\}\frac{L}{\beta^{\frac{m}{n-2}}} \tag{122}$$

Equation (122) is equivalent to Equation (19) of Reference [8]. The additive dimensionless positive new term is defined as

$$C = \frac{BS_{p\min}^{n-2}}{\sigma_p^n t_p} \tag{123}$$

(This term is equivalent to Equation (20) of Reference [8].) For fast unloading this is

$$C = \frac{\frac{B}{\sigma_p^2} - \frac{t_u}{n+1}}{t_p} \quad \text{when } t_u \le (n-2)\frac{B}{\sigma_p^2} \tag{124}$$

and for slow unloading this is

$$C = \frac{3}{(n+1)t_p}\left[\left(\frac{n-2}{t_u}\right)^{n-2}\left(\frac{B}{\sigma_p^2}\right)^{n+1}\right]^{\frac{1}{3}} \quad \text{when } t_u \ge (n-2)\frac{B}{\sigma_p^2} \tag{125}$$

At the fast/slow unloading transition point, one has the transitional value

$$C_0 = \frac{3}{n+1}\frac{B_0}{\sigma_p^2 t_p} = \frac{3}{(n+1)(n-2)}\frac{t_u}{t_p} \quad \text{when } t_u = (n-2)\frac{B_0}{\sigma_p^2} \tag{126}$$

B_0 is the transitional B-value of Equation (79). To obtain the above, Equation (69) for α and Equation (64) for t_p have been used.

By Equation (123), proof-testing ensures an inert strength exceeding

$$S_p \geq S_{p\min} = \left(\frac{\sigma_p^n t_p}{B} C\right)^{\frac{1}{n-2}} \tag{127}$$

(This agrees with Equations (72) and (78) for minimum surviving strength.) This, along with Equations (121), (118), and (120), gives the proof-testing mean break rate and reciprocal mean survival length as

$$N_p = \left[\frac{\sigma_p^n t_p}{\beta}(1+C)\right]^{\frac{m}{n-2}} = \frac{1}{L_p} \tag{128}$$

The β-value can be obtained from proof test parameters as

$$\beta = \frac{\sigma_p^n t_p (1+C)}{N_p^{\frac{n-2}{m}}} = \sigma_p^n t_p (1+C) L_p^{\frac{n-2}{m}} \tag{129}$$

Alternatively, the β-value can be obtained from fatigue testing, as in 11.7 and 11.8 below.

Unlike the situation of Equation (90) for inert strength without proof-testing, a post-proof-test Weibull plot is not linear. From Equation (122) such a plot has the slope

$$\text{slope}\,(S_p) = \frac{mCS_p^{n-2}\left(CS_p^{n-2} + S_{p\min}^{n-2}\right)^{\frac{m}{n-2}-1}}{\left(CS_p^{n-2} + S_{p\min}^{n-2}\right)^{\frac{m}{n-2}} - S_{p\min}^m (1+C)^{\frac{m}{n-2}}} \tag{130}$$

The effect of proof-testing is such that as the inert strength increases from the truncated value of Equation (127), the slope rapidly decreases from infinity to $n - 2$ and then towards m, the slope without proof-testing. For bimodal distributions at lower strengths, usually $m < n - 2$; at higher strengths, usually $m > n - 2$, according to Reference [9].

Note that as the proof test stress and effective proof test time go to zero, so does the minimum strength. The probability distribution of Equation (122) reduces to the linear form of Equation (86) before proof-testing.

11.7 Weibull analysis for static fatigue after proof-testing

The post-proof-test stress strength similar to Equation (57) is given by

$$S_p^{n-2} = \sigma_a^{n-2}\left(1+\frac{\sigma_a^2 t_{fp}}{B}\right) \tag{131}$$

Substituting this into the survival probability of Equation (122) gives the static Weibull distribution after proof-testing

$$\ln\frac{1}{P_p(t_{fp})} = \left\{\left[\left(t_{fp}+\frac{B}{\sigma_a^2}\right)\sigma_a^n + t_p\sigma_p^n\right]^{m_s} - \left[t_p\sigma_p^n(1+C)\right]^{m_s}\right\}\frac{L}{\beta^{m_s}} \tag{132}$$

From Equations (104) and (129),

$$\beta^{m_s} = B^{m_s} S_0^m L_0 = \frac{\left[\sigma_p^n t_p(1+C)\right]^{m_s}}{N_p} = \left[\sigma_p^n t_p(1+C)\right]^{m_s} L_p \tag{133}$$

In Equation (132) the numerator is zero for certain survival P_p = 1, so that proof-testing ensures a static fatigue failure time

$$t_{fp} \geq t_{fp\min} = t_p\left(\frac{\sigma_p}{\sigma_a}\right)^n C - \frac{B}{\sigma_a^2} \tag{134}$$

(This result can be obtained also directly from Equations (127) and (131).) With Equation (124) for fast unloading this becomes

$$t_{fp\min} = \left(\frac{\sigma_p}{\sigma_a}\right)^n\left(\frac{B}{\sigma_p^2} - \frac{t_u}{n+1}\right) - \frac{B}{\sigma_a^2} \quad \text{where } t_u \leq (n-2)\frac{B}{\sigma_p^2} \tag{135}$$

and with Equation (125) for slow unloading this becomes

$$t_{fp\min} = \frac{3}{n+1}\left(\frac{\sigma_p}{\sigma_a}\right)^n\left[\left(\frac{n-2}{t_u}\right)^{n-2}\left(\frac{B}{\sigma_p^2}\right)^{n+1}\right]^{\frac{1}{3}} - \frac{B}{\sigma_a^2} \quad \text{when } t_u \geq (n-2)\frac{B}{\sigma_a^2} \tag{136}$$

Unlike the situation of Equation (106) for static fatigue without proof-testing, a post-proof-test Weibull plot is not linear. The effect of proof-testing is such that, as the static fatigue failure time increases from the truncated value of Equation (134), the slope rapidly decreases from infinity to unity and then towards m_s (the slope without proof-testing). For bimodal distributions, at lower failure times, usually $m_s < 1$; at higher failure times, usually $m_s > 1$. As the proof test stress and effective proof test time go to zero, so does the minimum failure time. The probability distribution of Equation (132) reduces to the linear form of Equation (106) before proof-testing.

With C << 1, the result of Equation (132) and a less exact Equation (131) would be approximately equivalent to a result [B] given in Reference [19].

11.8 Weibull analysis for dynamic fatigue after proof-testing

The post-proof-test stress strength similar to Equation (58) is given by

$$S_p^{n-2} = \sigma_{fp}^{n-2}\left[1+\frac{\sigma_{fp}^3}{(n+1)B\dot{\sigma}_a}\right] \tag{137}$$

Substituting this into the survival probability of Equation (122) gives the dynamic Weibull distribution after proof-testing

$$\ln\frac{1}{P_p(\sigma_{fp})} = \left\{\left[\frac{\sigma_{fp}^{n+1}}{(n+1)\dot{\sigma}_a} + B\sigma_{fp}^{n-2} + \sigma_p^n t_p\right]^{\frac{m_d}{n+1}} - \left[\sigma_p^n t_p(1+C)\right]^{\frac{m_d}{n+1}}\right\}\frac{L}{\beta^{\frac{m_d}{n+1}}} \tag{138}$$

From Equations (111) and (129),

$$\beta^{\frac{m_d}{n+1}} = \frac{\left[\sigma_p^n t_p(1+C)\right]^{\frac{m_d}{n+1}}}{N_p} = \left[\sigma_p^n t_p(1+C)\right]^{\frac{m_d}{n+1}} L_p \tag{139}$$

In Equation (138) the numerator is zero for certain survival P_p = 1, so that proof-testing ensures a dynamic fatigue failure stress contained in

$$\frac{\sigma_{fp\min}^{n+1}}{(n+1)\dot{\sigma}_a} + B\sigma_{fp\min}^{n-2} = \sigma_p^n t_p C \tag{140}$$

(This result can be obtained also directly from Equations (127) and (137).)

If the minimum failure stress satisfies the inequality in Equation (108), then the approximate solution is

$$\sigma_{fp\min} \approx [(n+1)\dot{\sigma}_a \sigma_p^n t_p C]^{\frac{1}{n+1}} \tag{141}$$

With Equation (140) and Equation (124) for fast unloading this becomes

$$\sigma_{fp\min} \approx \left\{\sigma_a \sigma_p^n\left[(n+1)\frac{B}{\sigma_p^2} - t_u\right]\right\}^{\frac{1}{n+1}} \quad \text{when } t_u \le (n-2)\frac{B}{\sigma_p^2} \tag{142}$$

and with Equation (125) for slow unloading this becomes

$$\sigma_{fp\min} \approx \left\langle 3\sigma_a \left\{ \left[\frac{(n-2)\sigma_p}{t_u} \right]^{n-2} B^{n+1} \right\}^{\frac{1}{3}} \right\rangle^{\frac{1}{n+1}} \quad \text{when } t_u \geq (n-2)\frac{B}{\sigma_p^2} \tag{143}$$

Unlike the situation of Equation (113) for dynamic fatigue without proof-testing, a post-proof-test Weibull plot is not linear. The effect of proof-testing is such that as the failure stress increases from the truncated value of Equation (141), the slope rapidly decreases from infinity to $n + 1$ and then towards m_d (the slope without proof-testing). For bimodal distributions at lower failure stresses, usually $m_d < n + 1$; at higher failure stresses, usually $m_d > n + 1$. Note that as the proof test stress and effective proof test time go to zero, so does the minimum failure stress. The probability distribution of Equation (138) reduces to the linear form Equation (113) before proof-testing.

With C << 1, the result of Equation (138) and a less exact Equation (137) would be approximately equivalent to a result [A] given in Reference [19].

12 Reliability prediction

12.1 Reliability under general stress and constant stress

The theory given in the previous subclauses assumes that fibre crack parameters n and B do not change with time, although crack size a and strength S do change. Estimates of these parameters are obtained from the fatigue testing described in Clause 11. In addition to the items in 8.3, these estimates depend upon experimental conditions such as test duration, stress level, flaw initial strength, and environmental conditions. Careful and informed engineering judgement is required for reliability design.

In-service lifetime and in-service failure rate can be calculated for various fibre stress histories as follows. For a crack subjected to an arbitrary stress history to failure, the failure time is implicitly contained in the general lifetime Equations (39) and (40) or (42). In principle, Equation (45) or (46) could be used for lifetime prediction, since the intercept is directly obtained by static fatigue and Equation (47), or is indirectly obtained by dynamic fatigue and Equation (54). However, crack strengths are statistically distributed along the fibre length according to Equation (85). This means that the failure times or the equivalent failure rates must also be statistically distributed.

Examples of stress histories and geometries are constant tension, as in a buried cable or in a bend within a splice housing, or variable tension, as due to temperature cycles, wind, or fibre payout from a bobbin or reel. However, a fibre that is subjected to a time-invariant constant applied service stress is the commonest situation for which reliability calculations are made.

The preceding static fatigue probabilities explicitly contain failure time, so that lifetime may be extracted. As an alternative to lifetime, one may calculate the failure rate. The instantaneous value, derived from Equation (8) of Reference [20] and Equation (20) of Reference [21], is given by

$$\lambda_i(t_f) = \frac{\partial F}{P\partial t_f} = \frac{-\partial P}{P\partial t_f} \tag{144}$$

where F = 1 – P is the failure probability. An important special case applicable to Weibull distributions is

$$\lambda_i(t_f) = \frac{\partial zL}{\partial t_f} \text{ if } P \propto \exp(-zL) \text{ or } \ln\frac{1}{P} \propto zL \tag{145}$$

The averaged value is given by

$$\lambda_a(t_f) = \frac{F}{t_f} \tag{146}$$

In most practical cases the allowed failure probability of interest is small, so that

$$\ln\frac{1}{P} \approx F \text{ if } F < 10^{-3} \tag{147}$$

may be used in the formulae to within 0,5 % accuracy.

Reliability before proof-testing is of little interest, since virtually all commercial fibre has been proof-tested. If desired, results for the former may be obtained by letting the proof test stress and effective proof test time both go to zero. For simplicity, from this point on, we will drop the post-proof-test stress subscript p, except for the proof test stress σ_p and effective proof test time t_p.

Failure rate is a function of the lifetime and vice versa, and both can be expressed in terms of the survival probability. The most useful forms, given here, are lifetime as a function of failure probability and failure rate as a function of lifetime.

12.2 Lifetime and failure rate from fatigue testing

In terms of the static survival probability, the Weibull distribution of Equation (132) can be solved for the post-proof-test lifetime to give

$$t_f = \left\{ \left[\frac{\beta^{m_s}}{L} \ln\frac{1}{P} + \left(\sigma_p^n t_p\right)^{m_s} (1+C)^{m_s} \right]^{\frac{1}{m_s}} - \sigma_p^n t_p \right\} \sigma_a^{-n} - \frac{B}{\sigma_a^2} \tag{148}$$

(When C << 1, Equation (148), without $B\sigma_a^{-2}$, is equivalent to Equation (9) of Reference [20].)

Using Equation (132) gives the post-proof-test instantaneous failure rate of Equation (145) as

$$\lambda_i(t_f) = m_s L \left(\frac{\sigma_a^n}{\beta}\right)^{m_s} \left[t_f + t_p \left(\frac{\sigma_p}{\sigma_a}\right)^n + \frac{B}{\sigma_a^2} \right]^{m_s - 1} \text{ for } t_f \geq t_{f\min} \tag{149}$$

$$= 0 \text{ for } t_f \leq t_{f\min}$$

When C << 1, Equation (149), without $B\sigma_a^{-2}$, is equivalent to Equation (3) of Reference [21]. The failure rate scales linearly with fibre length. The minimum value of lifetime is given by

Equations (135) and (140); before this time has elapsed the instantaneous failure rate is zero and the survival probability is one. Then from Equation (149), the instantaneous failure rate jumps to

$$\lambda_{i\max} = m_s L \frac{\sigma_a^n}{\beta^{m_s}} \left[\sigma_p^n t_p (1+C)\right]^{m_s-1} \tag{150}$$

and the survival probability begins to decrease. The fractional rate of change of instantaneous failure rate with failure time is

$$\frac{d\lambda_i}{\lambda_i dt_f} = \frac{m_s - 1}{t_f + t_p \left(\frac{\sigma_p}{\sigma_a}\right)^n + \frac{B}{\sigma_a^2}} \quad \text{for } t_f > t_{f\min} \tag{151}$$

Hence after the minimum time, the failure rate decreases with failure time whenever static m_s < 1 or inert m < n – 2 from Equation (102), or dynamic m_d < n + 1 from Equation (114). With the non-linear Weibull distributions described in 11.2.2, this is usually the case in the lower strength extrinsic flaw region in the vicinity of proof-testing.

Using Equation (132) gives the post-proof-test averaged failure rate of Equation (146) as

$$\lambda_a(t_f) = \frac{1}{t_f}\left(1 - \exp\left\langle\left\{\left[\sigma_p^n t_p (1+C)\right]^{m_s} - \left[\left(t_f + \frac{B}{\sigma_a^2}\right)\sigma_a^n + \sigma_p^n t_p\right]^{m_s}\right\}\frac{L}{\beta^{m_s}}\right\rangle\right) \tag{152}$$

There is a singularity at zero time, and the rate is not exactly proportional to length.

12.3 Certain survivability after proof-testing

For "certain" survivability and the equations above, simplify. The lifetime of Equation (148) has its "guaranteed" minimum value of Equation (134). An alternate simple derivation may be used for this particular point in the Weibull distribution. From the "exact" static fatigue lifetime of Equation (45), the minimum lifetime is

$$t_{f\min} = B\left(S_{p\min}^{n-2} - \sigma_a^{n-2}\right)\sigma_a^{-n} \tag{153}$$

Then substitute Equations (72) and (78) for the minimum strength after proof-testing into this equation to obtain Equations (135) and (136).

Note that the minimum service lifetime is independent of fibre length and any m-value, but it increases very rapidly as the ratio of proof test stress to applied service stress. If the unloading time in Equations (135) and (136) is sufficiently small,

$$t_{f\min} \approx B\frac{\sigma_p^{n-2} - \sigma_a^{n-2}}{\sigma_a^n} \quad \text{where} \quad t_u << (n+1)\frac{B}{\sigma_p^2} \tag{154}$$

Sometimes a "rule of thumb" is invoked in which a particular lifetime is thought to be assured if the proof test stress is three or four times the long-term applied service stress. In this case, Equation (154) becomes

$$t_{f\,\min} \approx \frac{B}{\sigma_a^2}\left(\frac{\sigma_p}{\sigma_a}\right)^{n-2} \quad \text{or} \quad \frac{B}{\sigma_p^2}\left(\frac{\sigma_p}{\sigma_a}\right)^{n} \tag{155}$$

If the B-value is too small, the concept of assured minimum lifetime is better replaced by lifetime as a function of some small failure probability.

12.4 Failures in time

The failure rate of a component in FIT is defined as the number of failures per billion component hours. Here, the number of components corresponds to a length L km of fibre. If $f(h)$ is the cumulative number of failures as a function of the number of hours h, under either accelerated conditions in the laboratory or service conditions in the field, the instantaneous failure rate is

$$\lambda_i(h) = \frac{10^9\, df(h)}{dh}\ \text{FIT} \tag{156}$$

This is the slope of the curve at the point (h, $f(h)$), obtainable if data in the neighbourhood of the point is known. On the other hand, the averaged failure rate is

$$\lambda_a(h) = \frac{10^9 f(h)}{h}\ \text{FIT} \tag{157}$$

This is the slope of the straight line from the origin to the point (h, $f(h)$), obtainable from the data point alone.

Now relate these definitions to the formulae derived above, converting to failures per hour. Using Equation (149), the instantaneous failure rate in FIT is

$$\lambda_i(t_y) = 3{,}6\times 10^{12}\lambda_i(t_f) = 3{,}6\times 10^{12} m_s L\left(\frac{\sigma_a^n}{\beta}\right)^{m_s}\left[t_f + t_p\left(\frac{\sigma_p}{\sigma_a}\right)^n + \frac{B}{\sigma_a^2}\right]^{m_s-1} \tag{158}$$

Using Equation (152), the averaged failure rate in FIT is

$$\lambda_a(t_y) = 3{,}6\times 10^{12}\lambda_a(t_f)$$

$$= \frac{3{,}6\times 10^{12}}{t_f}\times\left(1-\exp\left\langle\left\{\left[\sigma_p^n t_p(1+C)\right]^{m_s} - \left[\left(t_f + \frac{B}{\sigma_a^2}\right)\sigma_a^n + \sigma_p^n t_p\right]^{m_s}\right\}\frac{L}{\beta^{m_s}}\right\rangle\right) \tag{159}$$

In both of these equations, there is the time conversion

$$t_f(\text{sec}) = 60 \times 60 \times 24 \times 365{,}25 \times t_y(\text{yr}) = 31\,557\,600\; t_y(\text{yr}) \quad (160)$$

For both failure rates, β must have the unit $\text{GPa}^n \cdot \text{s} \cdot \text{km}^{\frac{n-2}{m}}$. The unit of FIT comes from the value of L used in Equation (159), except in the case of bending, where the unit is L_B, from Equation (21).

13 *B*-value – Elimination from formulae, and measurements

13.1 Overview

In the survival probability, lifetime, and failure rate formulae of the previous parts, the B-value appears frequently. In this part, an outline of how it is measured is given, but there are as yet no agreed-upon methods. Fortunately, we will show how B can be neglected in these formulae to give worst-case estimates.

13.2 Approximate Weibull distribution after proof-testing

13.2.1 Overview

In this subclause, the "exact" results of Clause 10 and of 11.6 are related to approximations that have been used in the literature.

13.2.2 "Risky region" during proof-testing

As discussed in 10.4, the unloading time during proof-testing is important in determining the minimum surviving strength after proof-testing. In the slow-unloading region of 10.4.3, the strength can decrease indefinitely as the unloading time increases, but Reference [18] shows that the probability of this occurring is very small.

As a subset of the slow-unloading region, the "risky region" is defined as the region for which the strength after proof-testing drops below the proof test stress without fracturing. Referring to Equation (67), consider the strength $S_u(0)$ of a crack just before unloading. Defining the upper bound of the risky region, the maximum value of this strength is such that the strength $S_u(t_u)$ after proof-testing just equals the proof test stress σ_p. This gives the strength just before unloading to be

$$S_u(0) = \sigma_p \left[1 + \frac{\sigma_p^2 t_u}{(n+1)B} \right]^{\frac{1}{n-2}} \quad (161)$$

This is equivalent to Equation (23) of Reference [18]. Defining the lower bound of the risky region, the minimum value of the strength just before unloading is such that the strength $S_u(t_u)$ after proof-testing just equals the minimum strength given by Equation (78). This gives the strength just before unloading to be given by

$$S_u^{n-2}(0) = \frac{\sigma_p^n t_u}{(n+1)B} + \frac{3}{n+1}\left[\frac{(n-2)B\sigma_p}{t_u}\right]^{\frac{n-2}{3}} \quad (162)$$

This is equivalent to Equation (20) of Reference [18].

With longer unloading times, both the above limiting strengths before unloading increase. However, it is then shown that for a range of B-values and unloading times, the probability of finding a crack in the risky region is very small. This means that to a good approximation the minimum strength after proof-testing equals the proof test stress. Hence

$$S_{p\min} \approx \sigma_p \text{ and } C \approx C_a = \frac{B}{\sigma_p^2 t_p} \tag{163}$$

from Equation (123). (This approximation is equivalent to the expression after Equation (3) of Reference [18].)

13.2.3 Other approximations

Following after Equation (20) of Reference [8], simplification occurs if in Equation (122) the proof test stress and effective proof test time are large enough and the B-value is small enough that

$$S_{p\min}^{n-2} << \frac{\sigma_p^n t_p}{B} \approx S_{\min}^{n-2} \text{ or } C << 1 \tag{164}$$

using Equation (123). Note that with proof-testing, C may be small but never exactly zero. Then the results of 11.6 to 11.8 hold with C neglected.

Now make the further approximation

$$BS_p^{n-2} << \sigma_p^n t_p \tag{165}$$

(This is equivalent to the limit on $k_s \equiv BS_p^{n-2}$ after Equation (20) in Reference [8].) Then, with this approximation and C neglected, Equations (122) and (128) give

$$\ln \frac{1}{P_p(S_p)} \approx \frac{m}{n-2} L \frac{BS_p^{n-2}}{\beta^{\frac{m}{n-2}}} \left(\sigma_p^n t_p\right)^{\frac{m}{n-2}-1} \tag{166}$$

and

$$\ln \frac{1}{P_p(S_p)} \approx \frac{m}{n-2} N_p L \frac{BS_p^{n-2}}{\sigma_p^n t_p} \tag{167}$$

Equation (167) is equivalent to Equation (21) of Reference [8].

This summarizes the three limits used above in the sequence in which they usually occur

– characterizing the proof-testing

$$B << \sigma_p^2 t_p \tag{168}$$

– characterizing the dynamic fatigue testing

$$B << \frac{\sigma_f^3}{(n+1)\dot{\sigma}} \tag{169}$$

– characterizing the service conditions

$$B << \sigma_a^2 t_f \tag{170}$$

When these limiting approximations apply, then both B (apart from where it appears implicitly in β) and C can be neglected in essentially all formulae.

In the order of application, examine the numerical implications of these approximations using the parameter values of 6.5. Assume $a << b$ is equivalent to $a < 0{,}01b$.

- Equation (168): Taking the proof test stress to be between 0,35 GPa and 0,7 GPa, and the effective proof test time to be between 0,1 s and 1 s implies that $B < 1{,}2 \times 10^{-4}$ to $4{,}9 \times 10^{-3}$ GPa^2·s.
- Equation (169): Assume a failure stress equal to the nominal proof test stress and other values of 6.5. Then $B < 3{,}4 \times 10^{-5}$ GPa^2·s is implied. (This value is lowered with smaller proof test stresses and raised, perhaps several orders of magnitude, for smaller stress rates.)
- Equation (170): This limitation is usually less stringent than the one above, since the right side has a smaller applied stress (by perhaps a factor of 10 or more) but has a much longer desired lifetime.

In practice, the smaller of the B-values obtained in the first and third items will apply.

With the above approximations, the proof-testing mean break rate and reciprocal mean survival length of Equation (128) become

$$N_p = \left(\frac{\sigma_p^n t_p}{\beta} \right)^{\frac{m}{n-2}} = \frac{1}{L_p} \tag{171}$$

and, as in Equation (129)

$$\beta = \frac{\sigma_p^n t_p}{N_p^{\frac{n-2}{m}}} = \sigma_p^n t_p L_p^{\frac{n-2}{m}} \tag{172}$$

This can be expressed in terms of static and dynamic Weibull parameters via

$$\frac{m}{n-2} = m_s = \frac{m_d}{n+1} \tag{173}$$

using Equations (102) and (109). The static Weibull distribution of Equation (132) is

$$\ln \frac{1}{P_p(t_f)} = \left[\left(t_f \sigma_a^n + t_p \sigma_p^n \right)^{m_s} - \left(t_p \sigma_p^n \right)^{m_s} \right] \frac{L}{\beta^{m_s}} \tag{174}$$

The dynamic Weibull distribution of Equation (138) is

$$\ln\frac{1}{P_p(\sigma_f)} = \left\{\left[\frac{\sigma_f^{n+1}}{(n+1)\dot{\sigma}_a} + \sigma_p^n t_p\right]^{\frac{m_d}{n+1}} - \left(\sigma_p^n t_p\right)^{\frac{m_d}{n+1}}\right\}\frac{L}{\beta^{\frac{m_d}{n+1}}} \tag{175}$$

An alternative "simple" approach to one of these results is taken in Reference [22]. There Equation (7) (in the current notation) is

$$F_p = \frac{L}{L_p}\left[\left(1+\frac{\sigma_a^n t_f}{\sigma_p^n}\right)^{\frac{1}{n}} - 1\right] \tag{176}$$

This is used to calculate the ratio σ_p/σ_a of proof test stress to service stress as a function of fibre length L for several failure probabilities F_p and survival lengths L_p. Equation (166) is obtainable from Equations (174) and (172) with several approximations. First, the failure probability F_p is small as discussed at the beginning of Clause 7. Loading and unloading times of proof test are ignored, and the dwell time is 1 s, so that the failure time t_f must be measured in seconds or as a ratio to the dwell time. Most significantly, the Weibull parameter m_s does not appear in Equation (176), but is effectively replaced by $1/n$, so Weibull testing is not required in this approach. From Equation (173) this would imply that $m_d = 1 + \frac{1}{n}$, whereas in practice the dynamic Weibull parameter in the low-strength region is closer to 2,4 (see 6.5). Hence evaluations from Reference [22] and Equation (176) are questionable.

13.3 Approximate lifetime and failure rate

In this subclause, the approximations of Equations (168) and (169) are applied to the "exact" results of Clause 12.

Now Equation (148) for lifetime as a function of probability becomes

$$t_f = \left\{\left[\frac{\beta^{m_s}}{L}\ln\frac{1}{P} + \left(\sigma_p^n t_p\right)^{m_s}\right]^{\frac{1}{m_s}} - \sigma_p^n t_p\right\}\sigma_a^{-n} \tag{177}$$

This is equivalent to Equation (7) of Reference [18].

Similarly the failure rates in FIT as a function of time are

$$\lambda_i(t_f) = 3{,}6\times10^{12} m_s L\left(\frac{\sigma_a{}^n}{\beta}\right)^{m_s}\left[t_f + t_p\left(\frac{\sigma_p}{\sigma_a}\right)^n\right]^{m_s-1} \tag{178}$$

for the instantaneous rate from Equation (158), and

$$\lambda_a(t_f) = \frac{3{,}6\times10^{12}}{t_f}\left\langle 1-\exp\left\{\left[\left(t_p\sigma_p^n\right)^{m_s} - \left(t_f\sigma_a^n + t_p\sigma_p^n\right)^{m_s}\right]\frac{L}{\beta^{m_s}}\right\}\right\rangle \tag{179}$$

for the averaged rate from Equation (159).

The minimum lifetime t_{fmin} of Equations (135) and (136) is zero in this approximation, so actual failure rate values will therefore be somewhat smaller than the values computed. From Equation (151), the instantaneous failure rate now decreases with time as

$$\frac{d\lambda_i}{\lambda_i dt_f} = \frac{m_s - 1}{t_f + t_p\left(\frac{\sigma_p}{\sigma_a}\right)^n} \text{ for } t_f > 0 \tag{180}$$

Note that this fractional rate of decrease gets smaller with each increasing item and with a larger ratio of proof test stress to applied stress.

13.4 Estimation of the *B*-value

13.4.1 Overview

There are several methods of estimating B from measurements. They should be carried out with a sufficiently long fibre sample (long gauge length and many samples). This subclause is incomplete and under further study.

13.4.2 Fatigue intercepts

The B-value appears in the static fatigue failure time of Equation (46) and in the dynamic fatigue failure stress of Equation (51). The influence of static and dynamic fatigue data is reflected in the vertical intercepts $t_f(1)$ for static fatigue in Equation (47) and $\sigma_f(1)$ for dynamic fatigue in Equation (52). The intercepts are related by Equation (54), which gives the desired

$$B = \frac{t_f(1)}{S^{n-2}} = \frac{\sigma_f^{n+1}(1)}{(n+1)S^{n-2}} \tag{181}$$

The n-values are obtained from the linear slopes of the respective fatigue plots.

13.4.3 Dynamic fatigue failure stress

From a dynamic fatigue measurement of failure stress, Equation (60) gives

$$B = \frac{\sigma_f^3}{\left[\left(\frac{S}{\sigma_f}\right)^{n-2} - 1\right](n+1)\dot{\sigma}_a} \tag{182}$$

13.4.4 Obtaining the strength

The "inert strength" S is required in the above equations. Because of the exponent n – 2, any error in measuring the strength is greatly magnified in solving for the B-value. One measurement method is to use an "inert" environment as defined in 8.1, along with dynamic fatigue given in 9.3. As stated in 9.4.3, the dynamic fracture stress approaches the inert strength as the applied stress rate increases. Unique strength values are difficult to obtain by either method.

13.4.5 Stress pulse measurement

Suppose that a flaw is weakened (but not broken) according to Equations (36) and (37); call this a generalized proof test. Next, stress the flaw to failure according to Equations (39) and (40).

As a particular case, apply a "triangular" pulse consisting of a proof test stress σ_p with no dwell time and with equal magnitude $\dot{\sigma}$ of loading and unloading stress rates. From proof test Equations (63) and (64), a surviving flaw weakens from $S_p(0)$ to S_p, where

$$S_p^{n-2} = S_p^{n-2}(0) - \frac{2\sigma_p^{n+1}}{(n+1)B\dot{\sigma}} \tag{183}$$

Without pause, immediately subject the flaw to dynamic fatigue at the same stress rate. From dynamic fatigue Equation (50), the fracture stress σfp is given in

$$\sigma_{fp}^{n+1} = (n+1)B\dot{\sigma}\left(S_p^{n-2} - \sigma_{fp}^{n-2}\right) \tag{184}$$

Both equations combine to give

$$S_p^{n-2}(0) = \frac{\sigma_{fp}^{n+1} + 2\sigma_p^{n+1}}{(n+1)B\dot{\sigma}} + \sigma_{fp}^{n-2} \tag{185}$$

If σ_f is the (greater) failure stress without proof-testing, a flaw of initial strength $S(0)$ satisfies

$$S^{n-2}(0) = \frac{\sigma_f^{n+1}}{(n+1)B\dot{\sigma}} + \sigma_f^{n-2} \tag{186}$$

If two cracks of the same initial strength $S_p(0) = S(0)$ are fatigue-tested, one with and one without the stress pulse, one can solve for the B-value as

$$B = \frac{2\sigma_p^{n+1} - \left(\sigma_f^{n+1} - \sigma_{fp}^{n+1}\right)}{(n+1)\dot{\sigma}\left(\sigma_f^{n-2} - \sigma_{fp}^{n-2}\right)} \tag{187}$$

On the right side of this equation, all quantities are known from measurement.

13.4.6 Flaw growth measurement

Direct measurement of the crack velocity V at various levels of stress intensity K_I can theoretically lead to an estimate of the critical velocity V_c according to Equation (32). This value, in conjunction with estimates of the other parameters in Equation (35), can provide an estimate of B. This method is under study.

Annex A
(informative)

Statistical strength degradation map

The physical meaning of the formulae, which appears in Clauses 10 and 11, to predict the fibre reliability can be understood intuitively by introducing the statistical extension of the strength degradation map provided in [7]. A schematic diagram of the statistical strength degradation map is illustrated in Figure A.1 [23].

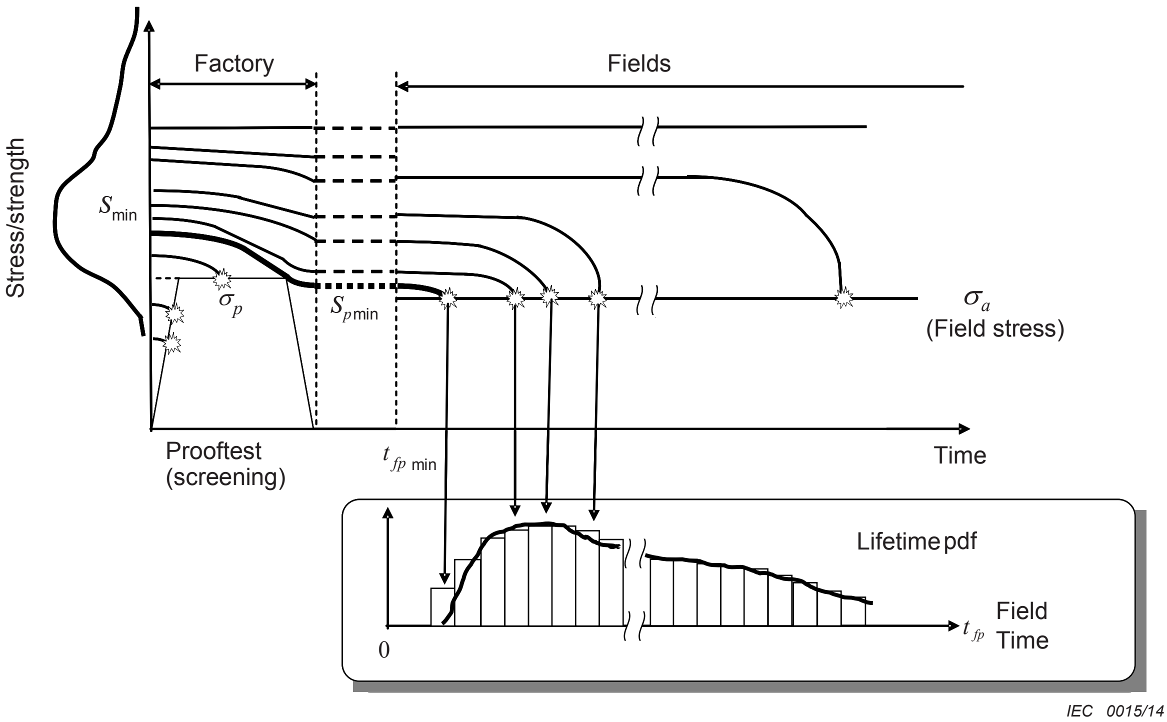

Figure A.1 – Schematic diagram of the statistical strength degradation map

In Figure A.1, the probability distribution attached to the vertical axis represents the fibre strength before proof-testing which approximately obeys the Weibull distribution (85). To reduce the "infant mortalities", the fibres require the proof-testing after drawing process under the nominally constant proof test stress σ_p. Note that, as shown in Clause 10, the loading and unloading condition of the test is restricted to avoid the unexpected crack weakening. The proof test stress generally degrades the fibre strength in accordance with the power law theory (Equation (34)) and some weaker fibres fail when the strength is equal or less than the proof test stress. The strength distribution of the surviving fibres S_p is calculated by using the conditional probability formula (116) and the minimum strength S_{pmin} is obtained by Equation (72) or (75). The surviving fibres will be provided in the field and undergo the applied stress σ_a. The fibre strength under the static stress is fatigued also in accordance with the power law theory. When the strength will coincide with or be less than the σ_a, the fibre fails. The lifetime of the fibre t_{fp} is derived by solving the Equation (131) after putting the S_p to σ_a. As shown in Figure A.1, since the lifetime t_{fp} strongly depends on the initial value of the S_p, t_{fp} is also statistically distributed and the survival probability is calculated as Equation (132). If $\sigma_a \geq \sigma_p$ holds, finite interval is necessary for occurring of the first failure of the weakest strength S_{pmin}. The no failure time t_{fmin} is calculated as shown in Equation (153).

The above discussions can be applied similarly to the case of the dynamic stress in the field and the several formulae shown in 11.8.

Bibliography

The limited references below are chosen mainly for their theoretical rather than experimental content. Portions of the above theory are found in many references, and the listing below is not meant to be exhaustive. Many more references, especially those containing experimental results, could have been included as background material but would not have substantially aided the theoretical development.

It is not necessary to read the references to be able to follow the development of this standard. The notation and terminology found in many references are varied and sometimes are inconsistent. In this technical report, both have been unified so that the theory can be read more easily.

[1] RITTER, John E. Jr., *Assessment of Reliability of Ceramic Materials* in *Fracture Mechanics of Ceramics*, vol. 5 *Surface Flaws, Statistics, and Microcracking* ed. by R. C. Bradt, A. G. Evans, D. P. H. Hasselman, F. F. Lange, pp. 227-251 (Plenum Press, N.Y., 1981)

NOTE A good summary of some theoretical aspects can be found in this standard as well as in the references listed therein.

[2] MALLINDER, F.P. and PROCTOR, B.A., *Elastic Constants of Fused Silica as a Function of Large Tensile Strain, Physics and Chemistry of Glasses*, vol. 5, pp. 91-103 (Aug. 1964)

[3] GLAESMANN, G.S. et al., *Effect of Strain and Surface Composition on Young's Modulus of Optical Fibers*, Proc. OFC '88, paper TUG5 (Jan. 1988)

[4] GRIFFIOEN, J., *Effect of Nonlinear Elasticity on Measured Fatigue Data and Lifetime Estimations of Optical Fibres,* Am. Ceramic Soc., vol. 75, pp. 2692-2696 (Oct. 1992)

[5] GLAESMANN, G.S., *Optical Fiber Failure Probability Predictions From Long-Length Strength Distributions,* Int'l. Wire and Cable Symp. Proc., pp. 819-825 (Nov. 1991)

[6] BREULS, A., *A COST 218 Comparison of n-Values Obtained with Different Techniques,* 2nd Optical Fibre Measurement Conference (OFMC '93), pp. 9-12 (Sept. 1993)

[7] FULLER, E.R. et al, *Proof Testing of Ceramics, Part 2 – Theory*, J. Materials Science, vol. 15, pp. 2282-2295 (1980)

[8] MITSUNAGA, Y. et al, *Failure Prediction for Long Length Optical Fiber Based on Proof Testing*, J. Applied Physics, vol. 53, pp. 4847-4853 (July 1982)

[9] BOGATYRJOV, V. A. *et al.*, *Mechanical Reliability of Polymer-Coated and Hermetically Coated Optical Fibers Based on Prooftesting* by Optical Engineering, vol. 30, pp. 690-699 (June 1991)

[10] GLAESMANN, G.S., *The Effect of Proof Testing on the Minimum Strength of Optical Fiber*, Int'l. Wire and Cable Symp. Proc., pp. 582-586 (Nov. 1991).

[11] MIYAJIMA, J., *Studies on High-Tensile Proof Tests of Optical Fibers*, J. Lightwave Technolgy, vol. LT-1, pp. 340-346 (June 1983).

[12] KURKI, J., STORMBOM, L., OKSANEN, L.,RÄSÄNEN, T. and LEINO, E., *Reliability and Environmental Performance of Cabled Single-Mode Optical Fibers,.* Int'l. Wire and Cable Symp. Proc., pp. 380-389 (Nov. 1989)

[13] Forms similar to this appear in many references. See, for example, reference [1].

[14] JOHNSON, C.A., *Fracture Statistics of Multiple Flaw Distributions*, in *Fracture Mechanics of Ceramics*, vol. 5 *Surface Flaws, Statistics, and Microcracking* ed. by R. C. Bradt, A. G. Evans, D. P. H. Hasselman, F. F. Lange, pp. 365-386 (Plenum Press, N.Y., 1981)

[15] PATEL, P.D. CHANDAN, H.C. and KALISH, D. *Failure Probability of Optical Fibers in Bending*, Int'l. Wire and Cable Symp. Proc., pp. 37-44 (Nov. 1981)

[16] MATTHEWSON, M.J. and KURKJIAN, C.R., *Static Fatigue of Optical Fibers in Bending*, J. Am. Ceramic Soc., vol. 70, pp. 662-668 (Sept. 1987)

[17] HELFINSTINE, J.D., *Adding Static and Dynamic Fatigue Effects Directly to the Weibull Distribution*, J. Am. Ceramic Soc., vol. 63, p. 113 (Jan. – Feb. 1980)

[18] GRIFFIOEN, W., *Evaluation of Optical Fiber Lifetime Models Based on the Power Law*, Optical Engineering, vol. 33, pp. 488-497 (Feb. 1994)

[19] *Proposal by the British Committee for Theory and Test Methods Determining Silica Fibre Strength*, IEC contribution 86A(United Kingdom)22 (Sept. 1990)

[20] TITCHMARSH, J.G., *Failure Rate as the True Parameter of Optical Fibre Reliability*, Int'l. Wire and Cable Symp. Proc., pp. 411-416 (Nov. 1992)

[21] LISLE, S.V., *A Failure Rate Approach for Predicting Optical Fiber Reliability*, OFC/IOOC'93 (Feb. 1993)

[22] MAZZARESE, Dave, WEIMANN, Peter, NORRIS, Richard and KONSTADINIDIS, Kariofilis, *Reliability Considerations for Next-Generation Bend-optimized Fibers,* Int'l. Wire and Cable Symp. Proc., (Nov. 2008)

[23] ASO, O., MATSUFUJI, T., ISHIKAWA, T., TADAKUMA, M., OTOSU, S., YAGI, T. and OKU, M., *Inference of the Optical Fiber Lifetime for Mechanical Reliability* by Furukawa Review, No. 42, pp.1-6 (Sep. 2012)

This page deliberately left blank

British Standards Institution (BSI)

BSI is the national body responsible for preparing British Standards and other standards-related publications, information and services.

BSI is incorporated by Royal Charter. British Standards and other standardization products are published by BSI Standards Limited.

About us

We bring together business, industry, government, consumers, innovators and others to shape their combined experience and expertise into standards -based solutions.

The knowledge embodied in our standards has been carefully assembled in a dependable format and refined through our open consultation process. Organizations of all sizes and across all sectors choose standards to help them achieve their goals.

Information on standards

We can provide you with the knowledge that your organization needs to succeed. Find out more about British Standards by visiting our website at bsigroup.com/standards or contacting our Customer Services team or Knowledge Centre.

Buying standards

You can buy and download PDF versions of BSI publications, including British and adopted European and international standards, through our website at bsigroup.com/shop, where hard copies can also be purchased.

If you need international and foreign standards from other Standards Development Organizations, hard copies can be ordered from our Customer Services team.

Subscriptions

Our range of subscription services are designed to make using standards easier for you. For further information on our subscription products go to bsigroup.com/subscriptions.

With **British Standards Online (BSOL)** you'll have instant access to over 55,000 British and adopted European and international standards from your desktop. It's available 24/7 and is refreshed daily so you'll always be up to date.

You can keep in touch with standards developments and receive substantial discounts on the purchase price of standards, both in single copy and subscription format, by becoming a **BSI Subscribing Member**.

PLUS is an updating service exclusive to BSI Subscribing Members. You will automatically receive the latest hard copy of your standards when they're revised or replaced.

To find out more about becoming a BSI Subscribing Member and the benefits of membership, please visit bsigroup.com/shop.

With a **Multi-User Network Licence (MUNL)** you are able to host standards publications on your intranet. Licences can cover as few or as many users as you wish. With updates supplied as soon as they're available, you can be sure your documentation is current. For further information, email bsmusales@bsigroup.com.

Revisions

Our British Standards and other publications are updated by amendment or revision.

We continually improve the quality of our products and services to benefit your business. If you find an inaccuracy or ambiguity within a British Standard or other BSI publication please inform the Knowledge Centre.

Copyright

Useful Contacts:

Customer Services
Tel: +44 845 086 9001
Email (orders): orders@bsigroup.com
Email (enquiries): cservices@bsigroup.com

Subscriptions
Tel: +44 845 086 9001
Email: subscriptions@bsigroup.com

Knowledge Centre
Tel: +44 20 8996 7004
Email: knowledgecentre@bsigroup.com

Copyright & Licensing
Tel: +44 20 8996 7070
Email: copyright@bsigroup.com

BSI Group Headquarters

389 Chiswick High Road London W4 4AL UK